Materials Horizons

ROYAL SOCIETY OF CHEMISTRY

REVIEW

View Article Online
View Journal | View Issue

Cite this: *Mater. Horiz.*, 2024, **11**, 5895

Visible-light-excited organic room temperature phosphorescence†

Longqiang Li,[ab] Depeng Liu,[ab] Jiayin Zhou,[ab] Min Qi,[ab] Guangqiang Yin *[ab] and Tao Chen *[abc]

Purely organic room temperature phosphorescence (RTP) materials have evoked considerable attention owing to their fantastic optical properties and broad application prospects. However, most of the reported organic RTP materials can be only excited by UV light, leading to accelerated photoaging of organic phosphors and severe lesions of organisms under excitation. In contrast to UV light, visible light (380–780 nm) has much lower phototoxicity, deeper penetrability and easier accessibility, which make visible-light-excited RTP materials more favorable for practical uses, especially for life-related applications. Although it remains greatly challenging to construct visible-light-excited RTP materials, impressive progress has been made with the rapid development of this field. Herein, we systematically outline the significant progress achieved in visible-light-excited RTP materials, including the design and construction strategies, unique properties, underlying mechanisms and their vital applications. In the final section, we highlight the current challenges and research perspectives for suggesting future studies of visible-light-excited RTP materials.

Received 8th July 2024,
Accepted 21st August 2024

DOI: 10.1039/d4mh00873a

rsc.li/materials-horizons

Wider impact

Most of the reported organic RTP materials can only be excited by UV light, greatly limiting their applications in bioimaging, photodynamic therapy, portable detection, *etc.* Therefore, it is highly urgent to develop efficient strategies for achieving visible-light-excited RTP materials. In this review, research advances in visible light-excited RTP materials are highlighted from construction strategies and optical properties to underlying emission mechanisms and innovative applications. With the rapid development of this field, several effective building strategies have been well established, including supramolecular aggregation and assembly, charge transfer, direct triplet state excitation and the formation of carbon dots. Benefiting from these reliable approaches, a myriad of visible light-excited high-performance RTP materials have been constructed, which are highly desirable and suitable for bioimaging, photodynamic therapy, information encryption, anti-counterfeiting, and portable detection. This review will not only benefit an in-depth understanding of the underlying construction principles and emission mechanisms of visible-light-excited RTP but also promote the development of this highly exciting field.

1. Introduction

Organic room temperature phosphorescence (RTP) materials have become one of the hot frontier directions in the fields of chemistry and materials science, due to their promising applications in bio-imaging, sensing, organic optoelectronics and so on.[1–11] Generally, the generation of organic RTP involves the following three main processes: (i) upon photoexcitation, the organic molecules are excited from the ground state (S_0) to the singlet excited state (S_n), and then transfer to the lowest singlet state (S_1) *via* rapid internal conversion (IC) according to Kasha's rule; (ii) the S_1 excitons undergo spin-flipping by the process of intersystem crossing (ISC) to the triplet excited state (T_n), followed by decaying to the lowest triplet state (T_1) through fast IC and (iii) finally, the T_1 excitons return to S_0 through the radiative phosphorescent transition (Fig. 1a). Early research mainly focused on heavy metal-related complexes, especially involving rare earth and transition metals with strong spin–orbit coupling (SOC) and high stability. However, these inorganic afterglow materials suffer from the issues of toxic heavy metals, terrestrial scarcities, high costs and harsh preparation conditions, *etc.* This motivates the development of purely organic RTP materials with fantastic advantages of abundant structural design, excellent biocompatibility, straightforward

[a] *Key Laboratory of Advanced Marine Materials, Ningbo Institute of Materials Technology and Engineering, Chinese Academy of Sciences, Ningbo 315201, China. E-mail: yinguangqiang@nimte.ac.cn, tao.chen@nimte.ac.cn*
[b] *School of Chemical Sciences, University of Chinese Academy of Sciences, Beijing 100049, China*
[c] *College of Material Chemistry and Chemical Engineering, Key Laboratory of Organosilicon Chemistry and Material Technology, Ministry of Education, Hangzhou Normal University, Hangzhou, 311121, Zhejiang, China*

† Dedicated to the 20th anniversary of the Ningbo Institute of Materials Technology and Engineering.

synthesis and cost-effectiveness.[12–17] However, organic RTP materials generally exhibit low quantum efficiency and short phosphorescent lifetime under ambient conditions due to the weak SOC and severe nonradiative transition. To address these intractable issues, several effective strategies have been developed, such as host–guest doping,[18–20] crystal engineering,[21–24] and aggregation,[25–27] leading to the mass emergence of high-performance organic RTP materials. These significant advances have greatly promoted the development of new-generation RTP materials and expanded innovative applications.

Although much impressive progress has been achieved, so far, most of the reported organic RTP materials can be only excited by near UV light (200–380 nm), largely limiting their practical applications, especially for bioimaging, phototherapy and portable sensing. Prolonged exposure to UV light may accelerate the photoaging of organic RTP materials and shorten the service life of the related devices. Moreover, strong UV light is associated with lesions and mutations in organisms. In contrast to UV light, visible light (380–780 nm) has lower phototoxicity, deeper penetrability and easy accessibility, which make it more favorable for practical applications.[28–30] Therefore, it is of great significance to develop visible-light-excited RTP. However, it remains a great challenge to realize visible-light-excited RTP mainly attributed to the following two factors. (i) The absorption of the most isolated organic phosphor is located in the UV light region. Although the extension of π-conjugation may redshift the absorption to the visible light region, it often leads to severe non-radiative dissipation from aggregation-induced quenching (ACQ) and violent molecular vibrations;[31] (ii) RTP materials that can be excited by visible light imply relatively lower excited state energy levels, in which excitons tend to return to the ground state *via* non-radiative transitions. Taken together, red-shifted absorption and effective inhibition of nonradiative dissipation are key prerequisites for achieving visible-light-excited RTP materials (Fig. 1a).

Despite the research on visible-light-excited organic RTP is still in its early stages, a series of significant advances have been achieved with the rapid development of this important field. However, no reported review introduces the development of the exciting field of visible-light-excited organic RTP. In this review, we aim to summarize and highlight the related research progress in recent years, focusing on the construction strategies, optical properties, underlying emission mechanisms, and applications of visible-light-excited RTP materials. To date, several effective construction strategies have been well established, including supramolecular aggregation and assembly, charge transfer, direct triplet state excitation and the formation of carbon dots (Fig. 1b). Benefiting from these feasible approaches, a myriad of visible-light-excited high-performance RTP materials have been constructed, which are highly desirable and suitable for bioimaging, photodynamic therapy, information encryption, anti-counterfeiting, and portable detection (Fig. 1c). At the end, a perspective discussion on the current challenges and prospects for future development will also be provided. We hope this review will spark new ideas, attract more research interests, and promote the development of this emerging field of visible-light-excited RTP.

Longqiang Li

Longqiang Li is a postgraduate in Ningbo Institute of Materials Technology and Engineering, Chinese Academy of Sciences. His current research interest focuses on the fabrication of visible-light-excited organic room temperature phosphorescence materials for application in information encryption and anti-counterfeiting.

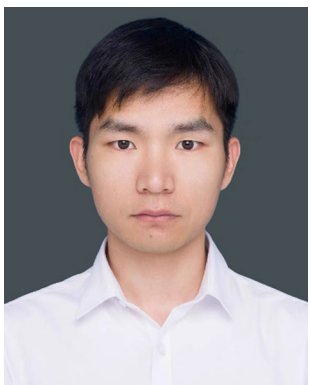

Guangqiang Yin

Dr Guangqiang Yin received his PhD degree from East China Normal University in 2019. He then joined Prof. Tao Chen's group as a postdoctoral research fellow at the Ningbo Institute of Materials Technology and Engineering (NIMTE), Chinese Academy of Sciences. His current research is focused on the design and construction of high-performance optical (smart fluorescence and organic ambient phosphorescence) materials by dynamic interactions for chemical sensing, information encryption and anti-counterfeiting applications.

Tao Chen

Prof. Dr Tao Chen (Fellow of the Royal Society of Chemistry, FRSC) received his PhD from Zhejiang University in 2006. After his postdoctoral training at the University of Warwick (UK), he joined Duke University (USA) as a research scientist. He then moved to Technische Universität Dresden (Germany) as an Alexander von Humboldt research fellow. Since 2012, he has been a full-time professor at the Ningbo Institute of Materials Technology and Engineering (NIMTE), Chinese Academy of Sciences. He has published more than 200 papers in the field of functional polymers. His research interests include smart optical materials, bioinspired actuators, photothermal composites and information storage.

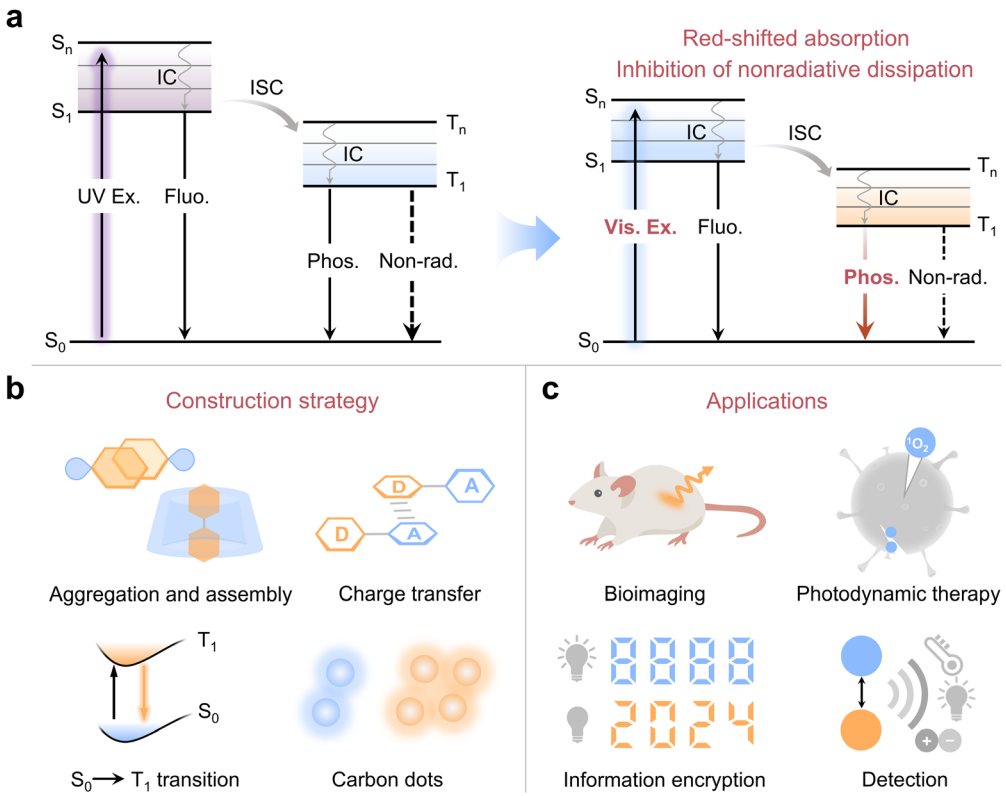

Fig. 1 (a) Simplified Jablonski diagram for interpreting organic RTP emission with excitation changing from the UV region to visible light. (b) The construction strategies for realizing visible-light-excited RTP materials. (c) The promising applications of the visible-light-excited RTP materials.

2. Design and construction of visible-light-excited RTP materials

In this section, we mainly summarize several effective strategies to construct visible-light-excited RTP materials following the design principles based on a bathochromic shift in absorption and suppression of non-radiative transitions. The primary construction strategies include supramolecular aggregation and assembly, charge transfer, direct triplet state excitation and the formation of carbon dots. Also, other methods such as multi-esterification and host–guest doping are introduced with several specific examples. The summarized construction strategies and the corresponding mechanisms will offer a better understanding of visible light excitation and benefit the development of visible-light-excited RTP materials.

2.1 Supramolecular aggregation and assembly

The aggregation and supramolecular assembly have been proved to be reliable and feasible strategies for preparing high-performance RTP materials.[32–34] Especially, the aggregation and assembly of fluorophores may redshift the absorption to the visible light region by intermolecular interactions, thus providing greater possibilities for realizing visible-light-excited RTP emission. The intermolecular interactions and molecular packing in aggregation have a significant impact on conjugation and energy levels, thereby being closely associated with their visible-light-excited properties.[35,36] Non-covalent intermolecular interactions regulate the molecular packing arrangements, and compact face-to-face packing is favorable for reducing the excited energy level and facilitating electron communication between neighboring molecules, which is highly beneficial for longer-wavelength excitation. In addition, the introduction of substituted groups can manipulate molecular packing modes, such as from edge-to-face to face-to-face packing. Moreover, the push–pull electron effect of the substituted groups can also alter the electron cloud density and change the conjugation degree. If the packing molecule comprises electron donors (D) and electron acceptors (A), it will form through-space charge transfer (TSCT) to extend conjugation, which contributes to realizing visible-light-excited RTP.

Huang and An *et al.* reported visible-light excited RTP materials using a family of halogen (Cl, Br)-modified aromatic amide derivatives by harnessing two collaborative channels (Fig. 2a).[37] On the one hand, halogen substituents enhanced ISC efficiency and tuned the molecular packing, resulting in a bathochromic shift of absorption. On the other hand, the excited triplet state can be stabilized by H-aggregation to achieve an efficient RTP emission. As a result, the resulting RTP materials can be excited by visible light, with a maximum excitation wavelength of up to 460 nm and the strongest excitation located at 410 nm. Therefore, the obtained RTP materials could be excited by mobile phone flashlights and incandescent light. In addition to visible-light excitation, the RTP materials show an ultralong lifetime of 0.84 s, along with a decent phosphorescence efficiency of 8.3%.

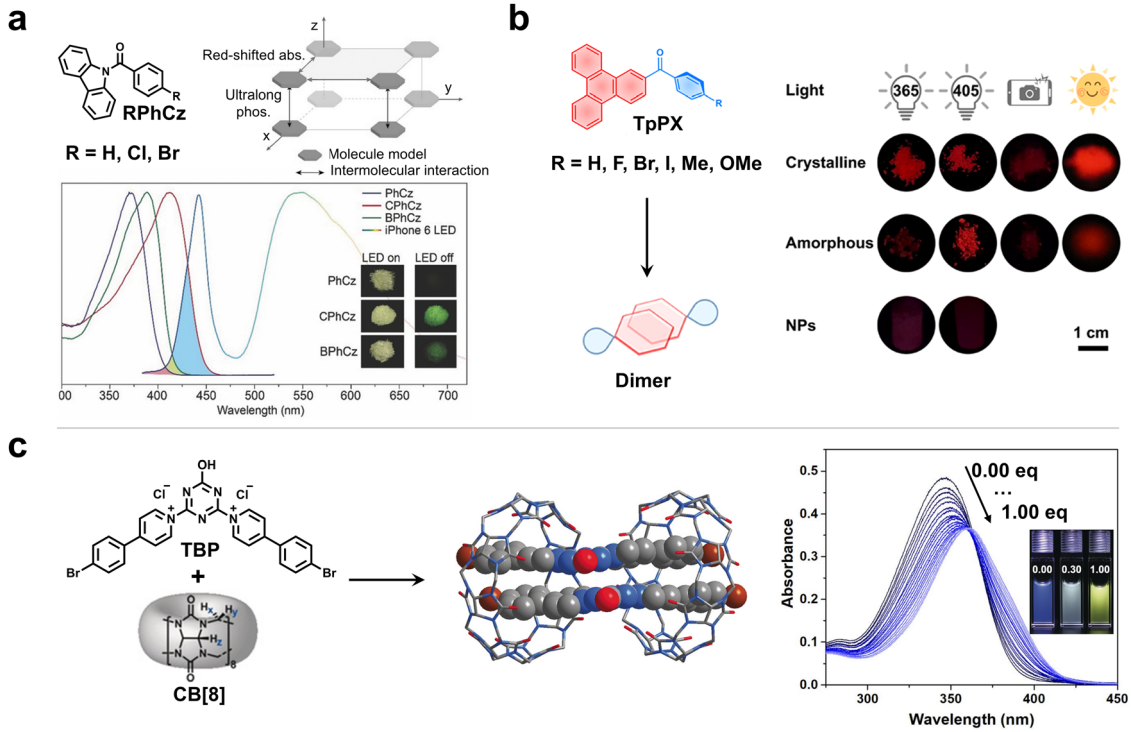

Fig. 2 (a) The realization of ultralong visible-light-excited RTP by the H-aggregation of aromatic amide derivatives. Reproduced with permission from ref. 37. Copyright 2017, Wiley-VCH. (b) The tightly dimeric luminophore enables effective excitation by different types of visible light. Reproduced with permission from ref. 38. Copyright 2024, The author(s). (c) The macrocyclic assembly of CB[8] and TBP to obtain a visible-light-excited host–guest inclusion complex. Reproduced with permission from ref. 39. Copyright 2019, Wiley-VCH.

Recently, Chi and Yang *et al.* reported a series of robust visible-light-excited RTP materials by using phenyl(triphenylen-2-yl)methanone RTP compounds possessing a typical large π-conjugated plane (Fig. 2b).[38] The strong π–π interactions caused by triphenylene cores promote the formation of tight dimers, which immensely suppress the nonradiative transitions, realizing robust deep-red RTP emission even in an amorphous state or under warm-damp conditions. More importantly, the aggregation effectively reduces excited energy levels and promotes the redshift of absorption/excitation, resulting in a wide range of excitations from 390 to 560 nm.

In addition to the small molecule systems, Zhang and coworkers developed visible-light-excited near-infrared (NIR, λ_{em} > 650 nm) RTP materials by regulating the molecular aggregates of naphthalenediimide (NDI) phosphors in the polymeric systems.[40] NDI was covalently introduced in the middle of the polymer chains of polylactide (PLA) and polycaprolactone (PCL), resulting in site-isolation of NDI aggregates to offer broadband visible-light absorption (450–650 nm). Interestingly, Zhang and coauthors obtained visible-light-excited and excitation-dependent ultralong RTP materials by regulating anionic cellulose trimellitate (CBtCOONa) aggregates.[41] The size of aggregates can be subtly modulated by the coordination bonds between COO^- and Ca^{2+}. With the increment of the aggregates, the absorption in the visible-light region gradually increases, leading to visible-light excitable RTP. Upon turning off the visible light, green or yellow afterglow can be observed by the naked eye.

Apart from aggregation, the supramolecular assembly of organic fluorophores with macrocyclic hosts *via* host–guest interactions is also an effective approach for accessing high-performance RTP materials. Among numerous excellent RTP materials that are produced by host–guest interactions, visible-light excitable RTP materials are still rare. Previously, Yong *et al.* reported three β-cyclodextrin (β-CD) inclusion complexes that presented excitation-dependent RTP emission.[42] As the excitation changed from UV to visible light (λ_{ex} = 425 or 460 nm), the RTP color of the complexes changed from blue to green. In 2014, the same group obtained a visible-light-excitable RTP material with a lifetime of microseconds that displayed similar light-responsive behavior by encapsulating other dye molecules within β-CD.[43] Impressively, Ma and Tian *et al.* reported visible-light-excitable RTP materials in an aqueous medium by leveraging cucurbit[8] (CB[8]) as a confined cavity to encapsulate triazine derivative (TBP) (Fig. 2c).[39] Specifically, a structure-restricted dimer of TBP could be formed within the rigid cavity of CB[8] to produce a charge-transfer triplet state. With the addition of CB[8], the absorption peak gradually extends to the visible-light region, enabling yellow RTP emission located at 565 nm in an aqueous solution under excitation at 405 nm.

2.2 Charge transfer

Molecules combined with D and A present an intramolecular or intermolecular charge transfer (CT) effect, generally enabling a significant bathochromic shift in absorption to the visible light

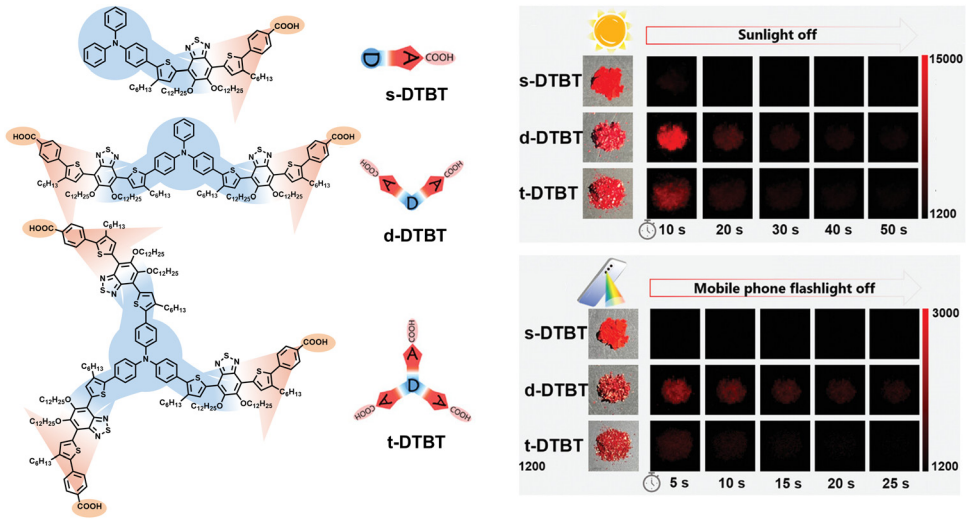

Fig. 3 Organic phosphors with different D–A branches enable efficient red RTP emission that can be excited by sunlight and the flashlight of a mobile phone. Reproduced with permission from ref. 29. Copyright 2022, Wiley-VCH.

region. Therefore, the introduction of the D–A design for the organic phosphors is highly conducive to obtaining visible-light-excited RTP materials. Importantly, Li *et al.* achieved a series of bright red RTP materials with a lifetime of up to 344 ms, which can be effectively excited by sunlight and flashlight of a mobile phone, through the rational combination of numbers and geometries of D and A units (Fig. 3).[29] It involves utilizing triphenylamine as D and benzothiadiazole as A, and incorporating carboxylic acid to enhance intermolecular interactions. Based on the D–π–A molecular design, the absorption of an ultralong RTP material largely extends to 600 nm due to the strong intramolecular CT effect, enabling high-performance visible-light-excited RTP emission located in the region of 630–660 nm.

Also by taking advantage of the D–A design, An and coworkers reported a series of visible-light-excitable RTP molecules by integrating the carbazolyl group with a σ-aromatic carboranyl cage (Fig. 4a).[44] Owing to strong intramolecular CT boosted by a σ-aromatic boron cluster, these carborane-based phosphors could be effectively excited by visible light in the region of 400–480 nm, along with a satisfactory RTP lifetime of up to 0.666 s. Besides, Ma and Tian *et al.* prepared visible-light-excited NIR RTP materials by copolymerization of acrylamide and monoiodo or diiodo substituted boron dipyrromethene

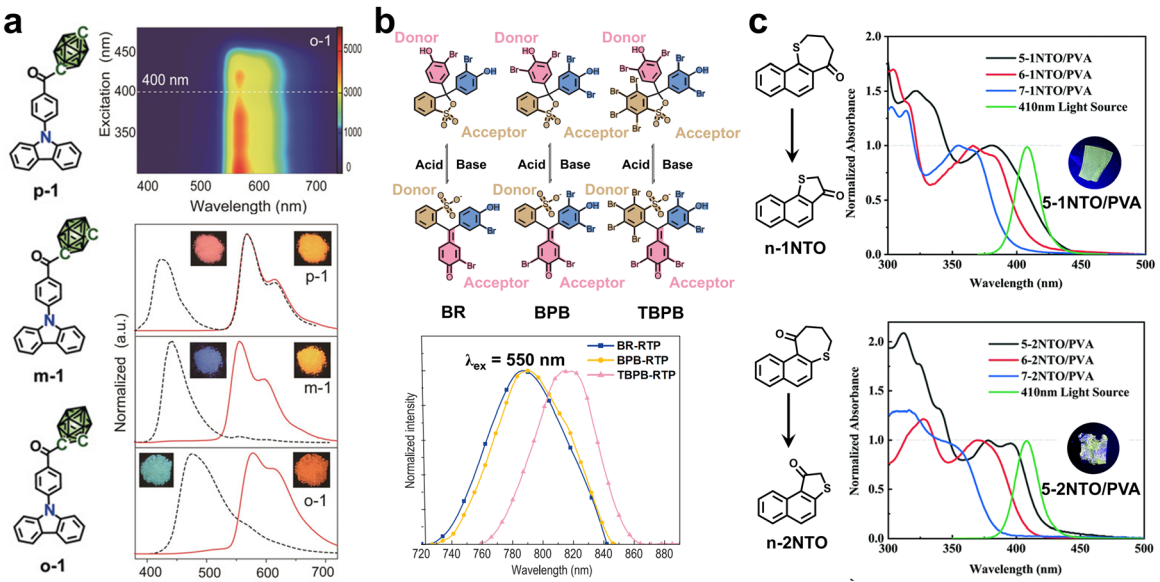

Fig. 4 (a) The carborane-based RTP materials with a D–A structure that are excitable by visible light. Reproduced with permission from ref. 44. Copyright 2019, Wiley-VCH. (b) The pH-responsive NIR RTP materials can be excited by green light (550 nm). Reproduced with permission from ref. 46. Copyright 2021, The author(s). (c) Shrinking the heterocycle from a seven-membered to a five-membered ring to promote intramolecular CT for realizing visible-light excited RTP. Reproduced with permission from ref. 47. Copyright 2021, Royal Society of Chemistry.

(Bodipy).[45] The as-prepared amorphous polymers displayed NIR RTP emission at 770 nm under excitation at 520 nm or 540 nm. Later, the same group further developed a set of visible-light-excited NIR RTP films by integrating PVA with phenolsulfonephthaleine derivatives with D–A design (Fig. 4b).[46] Notably, the obtained films could be excited by red light, displaying the reddest RTP emission at 819 nm and a maximum phosphorescent quantum yield (Φ_P) of up to 3.0%. Interestingly, the switch of RTP emission can be controlled by pH based on the regulation of open/closed ring states in molecule structures.

Besides, a bathochromic shift of the absorption could be realized by subtle structural design. Ma and coworkers reported a series of visible-light-excited RTP materials by doping naphthalene-based thiochromanone analogues (*n*-1NTO and *n*-2NTO, *n* = 5, 6, and 7) into the PVA matrix (Fig. 4c).[47] It was found that the absorption of these organic phosphors displayed a significant bathochromic shift upon shrinking the size of the heterocycle from a seven-membered ring to a five-membered ring. Such a phenomenon could be attributed to the large enhancement of intramolecular CT in a smaller and more planar heterocycle, originating from more p–π conjugation between the S atom and the naphthalene unit. As a result, the absorption of 5-1NTO@PVA and 5-2NTO@PVA could extend to 450 nm, leading to visible-light-excited RTP.

Except for intramolecular CT, Zheng *et al.* reported visible-light-excited RTP molecules that could be realized by intermolecular TSCT (Fig. 5a).[48] They designed and synthesized a visible-light-excited RTP phosphor, namely, CzSO, by attaching the 9,9-dimethylthioxanthene *S*,*S*-dioxide (SO) acceptor to the carbazolyl group. By taking advantage of TSCT, CzSO exhibited blue-light-excitable RTP with a long-lived lifetime of 0.45 s and a decent Φ_P of more than 26% under excitation at 440 nm. In addition, intense two-photon excited RTP could be realized upon excitation at 840 nm attributed to ground state CT. Also by leveraging intermolecular CT, Lin and coworkers developed a red RTP crystal that could be excited by visible light at 502 nm.[49] The crystal of 3,6-dibromophenanthrene-9,10-dicarbonitrile (BrPCN) cultivated from a hot solution of DMF revealed a red RTP emission at 615 nm when excited at 502 nm, accompanied by a Φ_P of 4.56% and a lifetime of 2.24 ms. The detailed experimental results and theoretical simulations jointly proved that a guest molecule named 3-bromo-6-(dimethylamino)phenanthrene-9,10-dicarbonitrile (NPCN) was produced during the crystallization of BrPCN host molecules to form a cocrystal. Consequently, the effective intermolecular CT between the host and the guest resulted in the red RTP and visible-light excitation.

Interestingly, Ray and Bhatia designed and synthesized a family of twisted RTP emitters by covalently attaching 2-chlorophenoxy, 2-fluorophenoxy, and 2-methoxy-phenoxy groups to the terephthalonitrile core, namely, TOC, TOF, TOM, respectively (Fig. 5b).[50] Compared with the dim afterglow of TOC and TOF, efficient RTP emission could be observed for TOM under visible light excitation. This result was attributed to a significant bathochromic shift of the absorption due to the strong electron-donating effect of methoxy groups in TOM. Impressively, An *et al.* summarized great advancements in manipulating intermolecular interactions for realizing high-performance RTP materials.[36] Manipulating intermolecular interactions (π–π interactions, n–π interactions, halogen bonding, and so on) can not only suppress the non-radiative transitions of excitons but also promote electronic communications among neighboring molecules, which is instructive for regulating intermolecular CT to realize visible-light-excited RTP.

Based on the intramolecular and intermolecular CT effects, strikingly, Wu and Chen *et al.* presented visible- and NIR-light excitable RTP nanoparticles in water by assembling difluoroboron β-diketonate compounds (BF_2bdk) (Fig. 6a).[28] It was

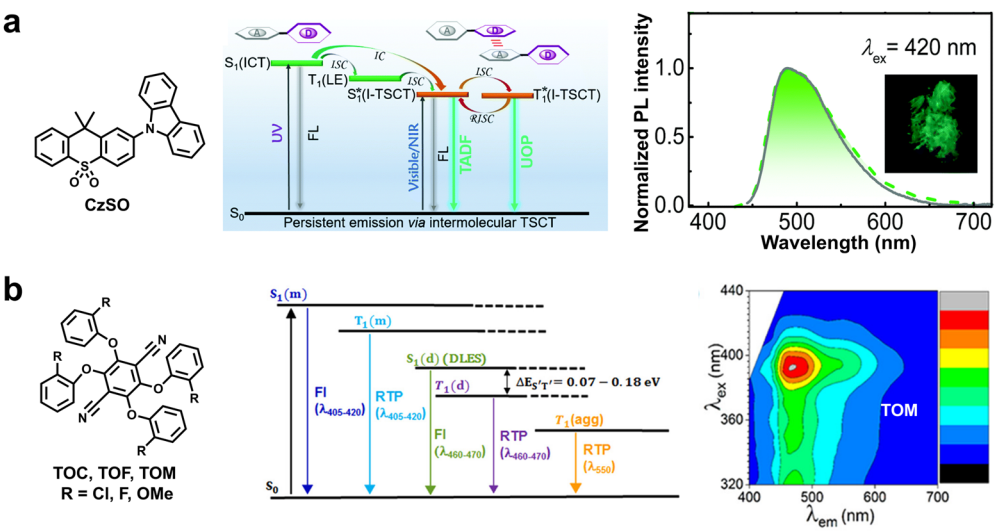

Fig. 5 (a) The formation of intermolecular through-space CT to achieve efficient visible-light-excited RTP. Reproduced with permission from ref. 48. Copyright 2020, Royal Society of Chemistry. (b) The terephthalonitrile derivatives exhibit multi-mode emissions and can be excitable by visible light. Reproduced with permission from ref. 50. Copyright 2019, American Chemical Society.

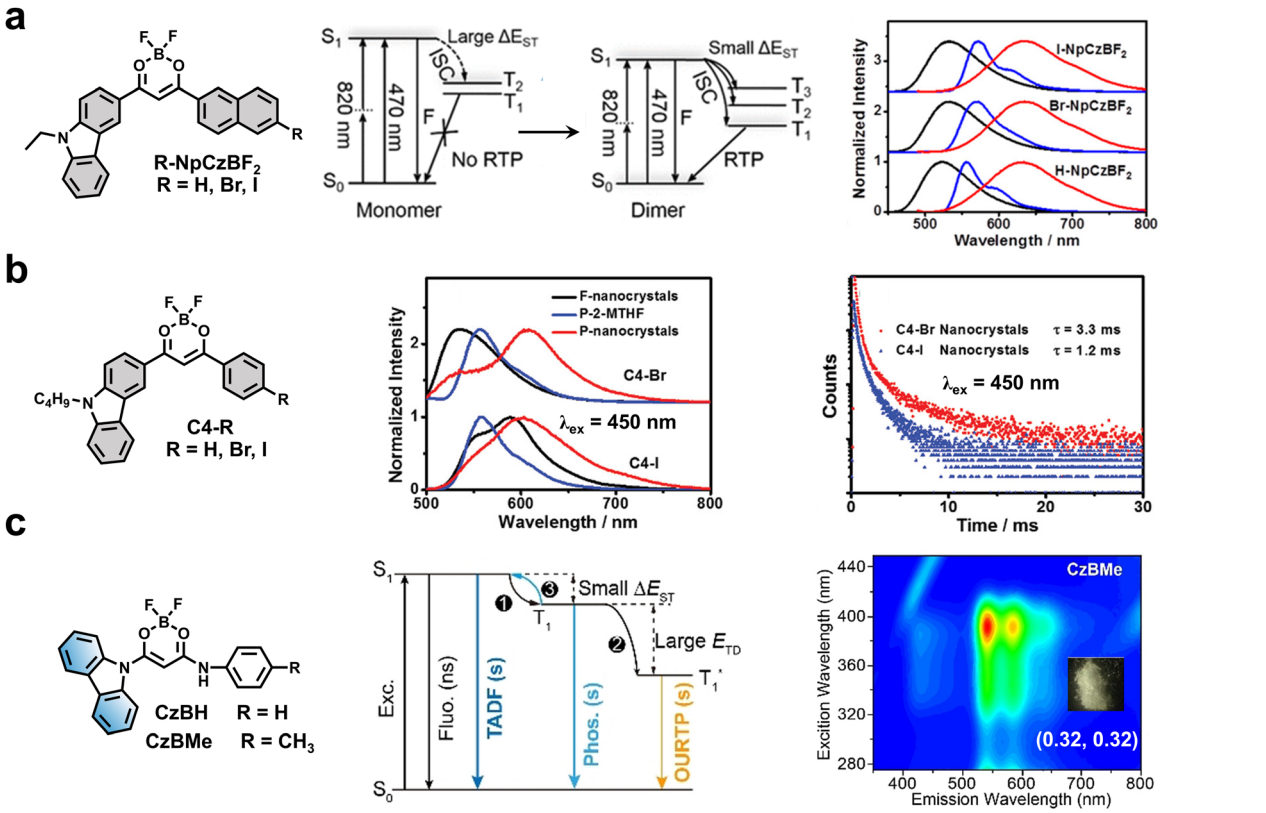

Fig. 6 (a) Visible- and NIR-light-excited RTP that combined with a difluoroboron β-diketonate unit (A) and a carbazolyl group (D). Reproduced with permission from ref. 28. Copyright 2019, American Chemical Society. (b) The D–A fluorogens for assembling visible-light-excited RTP nanocrystals, λ_{ex} = 450 nm. Reproduced with permission from ref. 51. Copyright 2020, Wiley-VCH. (c) The single-component D–A fluorogens enable white afterglow emission based on tri-mode emission. Reproduced with permission from ref. 52. Copyright 2021, Wiley-VCH.

found that the strong CT from D (carbazolyl group) to A (BF_2bdk) should be responsible for the redshift in the absorption of the organic phosphor to the visible light region. In addition, the formation of dimers promotes the ISC process by reducing singlet–triplet splitting energy (ΔE_{ST}). As a result, RTP emission centered at around 630 nm could be observed upon blue light irradiation at 470 nm. Later, the same group reported visible-light-excitable RTP nanocrystals through the micelle-assisted assembly of D–A fluorophores with the carbazolyl group as D and halogenated BF_2bdk as A (Fig. 6b).[51] Notably, the assembled nanocrystals displayed RTP at around 600 nm with a lifetime of more than 3 ms in water under excitation at 450 nm. Both experimental results and theoretical calculations unveiled that the molecular packing, halogen atoms and intermolecular interactions should be responsible for the RTP properties of the assembled nanocrystals.

White light-emitting materials have attracted considerable attention due to their fundamental significance and broad potential applications. Compared to the multicomponent white-light emitters, single-component white light-emitting materials have more advantages including less phase separation, low cost, and stable composition. Importantly, Huang *et al.* reported single-component visible-light-excitable white-light-emitting afterglow crystals based on tri-mode emission by the radiative transitions of S_1, T_1, and T_1^* (Fig. 6c).[52] The white afterglow with a Φ_P of 14.1% and a long lifetime of 0.61 s was realized by regulating the intensity ratios of each emitting component *via* modulating the singlet–triplet energy level and the exciton trapping depth. In the same year, Yang and Xue *et al.* also reported a white-emitting RTP molecule, namely DCBN, by introducing two carbazolyl groups onto benzonitrile.[53] Impressively, regardless of excitation wavelengths (300–520 nm), such twisted D–A molecules combined dual emission of RTP and thermally activated delayed fluorescence (TADF) to offer white light delayed emission, revealing a high efficiency (Φ > 6%) and a long lifetime (τ > 800 ms).

2.3 Direct triplet state excitation

To achieve phosphorescence emission, the transition of electrons from S_0 to S_n is usually necessary, followed by the relaxation from S_n to S_1 *via* fast IC, and ultimately transfer to T_n by ISC. Due to the high energy level of S_n, the excitation of most RTP materials is generally limited to high-energy light in the UV region. If it can bypass the ISC process, that is, directly exciting the phosphors from S_0 to T_n, it is anticipated that a distinct redshift of excitation to the region of visible light may be successfully realized (Fig. 7a). This innovative strategy redshifts the excitation wavelength by eliminating the involvement of high-lying S_n and unwanted relaxation processes, enabling efficient visible-light excited RTP systems.

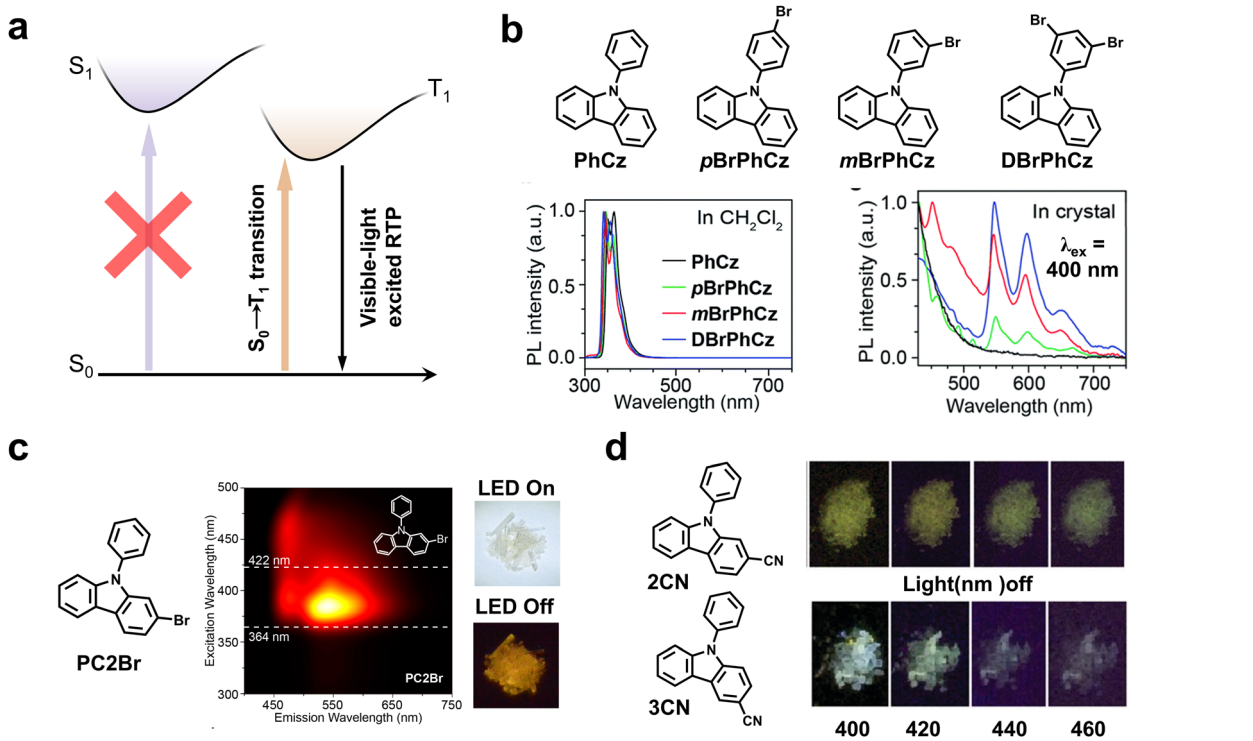

Fig. 7 (a) Simplified Jablonski diagram for interpreting the direct population of T_1 through $S_0 \rightarrow T_1$ transition. (b) The utilization of the heavy-atom effect for realizing RTP under excitation at 400 nm. Reproduced with permission from ref. 54. Copyright 2019, Royal Society of Chemistry. (c) The LED excitable RTP using Br-substituted aromatic molecules as phosphors based on direct $S_0 \rightarrow T_1$ transition. Reproduced with permission from ref. 55. Copyright 2024, The author(s). (d) RTP emission of CN-substituted carbazole derivatives under excitation at different visible lights. Reproduced with permission from ref. 56. Copyright 2019, Royal Society of Chemistry.

In 2019, Huang and Chen *et al.* reported a series of afterglow molecules with the ability to directly populate triplet excitons from $S_0 \rightarrow T_1$ transition by introducing bromine atoms into 9-phenyl-9*H*-carbazole (PhCz) (Fig. 7b).[54] With the combined effects of the heteroatom incorporation and molecular interactions, the $S_0 \rightarrow T_1$ transition was significantly enhanced to render a prolonged lifetime of up to 250 ms and an improved Φ_P of 9.5% under visible-light excitation at 400 nm. Recently, the same group further demonstrated the direct population of triplet excited states by using the similar molecular design (Fig. 7c).[55]

Also, Yang and Sun *et al.* designed and synthesized five D–A isomers of cyano-phenylcarbazoles that can be excited by 400–460 nm visible light (Fig. 7d).[56] Particularly, 2CN and 3CN with cyano groups modified on the 2- and 3-positions of the carbazolyl group showed enhanced visible-light-excitable RTP owing to H-aggregation by strong π–π stacking interactions. Based on the fluorescence and RTP excitation spectra, they deduced that the direct absorption of $S_0 \rightarrow T_1$ might be responsible for the visible-light excitation because the visible light of 440 and 460 nm could not excite $S_0 \rightarrow S_n$ transition in such small-sized conjugated molecules. In spite of high efficiency of such a strategy, Liu *et al.* reported that the impurities of the commercial carbazole have a significant influence on phosphorescence performance.[57] Therefore, more evidence should be provided for ruling out the potential impact of impurities on the strategy of direct triplet state excitation.

In addition to single molecular systems, Kimball *et al.* discovered that an indole@PVA film could be directly excited to triplet excited states under visible-light excitation at 405 nm.[58] The indole@PVA film could be excited at 290 nm and 405 nm with similar spectral characteristics. However, the phosphorescence anisotropy excited at 405 nm and 290 nm was positive and negative, respectively, indicating that a lower excited wavelength was involved in the standard excitation route and a longer excited wavelength was related to the direct $S_0 \rightarrow T_1$ absorption.

2.4 Carbon dots

Carbon dots (CDs) are zero-dimensional carbon nanomaterials that have received considerable attention due to their excellent properties such as low cost, relative innocuity and easy preparation.[59–61] Among diverse phosphorescent materials, CDs are especially easier to realize efficient visible-light-excited RTP, attributing to three main factors including (i) the increase of the conjugation degree caused by the size effect;[62,63] (ii) the change of the electronic structure and surface chemical activity caused by heteroatom-doped CD cores;[64,65] and (iii) the enhancement of intramolecular CT originating from abundant functional groups of electron donors and acceptors.[66,67] The excellent optical properties of CDs motivated us to summarize related advancements in recent years.

At present, CD-based RTP materials are generally prepared by embedding organic phosphors in various matrices including boron oxide (B_2O_3), boric acid (BA), silica gel, polyacrylamide (PAM), polyvinyl alcohol (PVA), polyurethane, *etc.* The rigid matrices provide rigid microenvironments for stabilizing triplet

excitons by minimizing energy dissipation, resulting in high-performance RTP emissions. In 2020, Wang and coworkers synthesized green emissive CDs (G-CDs) *via* hydrothermal pyrolysis of rhodamine B and embedded the as-obtained G-CDs into a B_2O_3 matrix, offering a visible-light-excited composite with a dual-mode afterglow of RTP and TADF (Fig. 8a).[68] Importantly, G-CDs@B_2O_3 could be excited by visible light sources such as a cellphone and an electric torch light, displaying an ultralong afterglow duration of about 13 s after the removal of the excitation source. Moreover, Sun and coworkers developed visible-light-excited multicolor afterglow composites using a similar method of embedding CDs into the B_2O_3 matrix.[69] Multiple afterglow colors varying from blue-green to orange-yellow could be obtained, accompanied by visible afterglow durations of several seconds after switching off the visible light.

Besides, Yan and coworkers obtained visible-light-excited dual-mode afterglow by embedding rose bengal (R) CDs in a BA matrix.[71] The as-prepared R-CDs@BA afterglow material exhibited yellow afterglow emission with an ultralong duration of over 5 s upon turning off the visible light. Notably, Qu and coauthors reported visible-light-excitable CD-based RTP materials (g-t-CD@BA) with an ultrahigh efficiency of 48% through a grinding-induced transition of the mixture (lycorine hydrochloride CDs and BA) from the amorphous to the crystallization state.[72] Impressively, g-t-CD@BA exhibited bright green RTP lasting for more than 9 s even after the excitation of sunlight on a cloudy day. Recently, Li and coworkers also harnessed BA as a matrix to prepare visible-light-excited CDs-based RTP composites (Fig. 8b).[70] The RTP composites were prepared by a one-step hydrothermal synthesis in the presence of BA and using amino acids as carbon sources. These CD-based RTP composites exhibited tunable afterglow emissions ranging from cyan to red depending on the types of carbon source, under visible light excitation at 420 nm. Notably, these CD-based RTP composites revealed excellent Φ_P of up to 54.27% and a maximum lifetime of 530 ms.

The polymer-based RTP materials have attracted considerable attention due to their excellent flexibility, good biocompatibility and processability. Doping CDs into a polymer matrix is an effective method for obtaining high-performance polymer-based RTP materials. In 2023, Chen and coworkers reported a series of polymer-based visible-light-excited RTP materials by doping four kinds of CDs into PAM.[73] Full-color RTP emissions including blue, green, yellow and red could be observed by the naked eye after turning off the flashlight. In the same year, Lv and coworkers prepared five different CDs by using 1,10-phenanthroline-5-amine (Aphen), citric acid and glucose as the carbon and nitrogen sources.[74] By doping them into PVA, the obtained films exhibited a high RTP efficiency of 36.7% and a long lifetime of 352.9 ms under excitation at 405 nm. Recently, Yuan and Wang *et al.* reported a record-long visible-light-excited RTP material by embedding nitrogen-doped CDs (N-CDs) into the PVA matrix (Fig. 8c).[65] Notably, the RTP lifetime of the obtained N-CDs@PVA reached up to 2.1 s under excitation at 420 nm, which was challenging for conventional visible-light-excited RTP materials. A strong yellow afterglow lasting for more than 5 s could be observed by the naked eye after irradiating with a common white-light-emitting diode (WLED). In addition, the N-CDs@PVA film displayed excitation wavelength-dependent RTP emission, showing a distinct red shift from green to yellow upon varying the excitation wavelength from 254 to 470 nm.

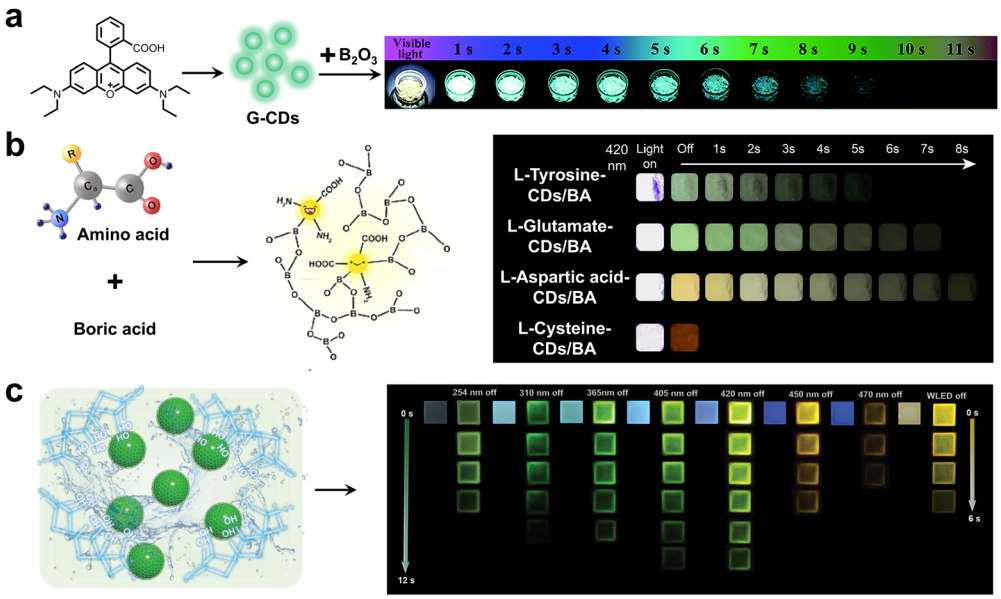

Fig. 8 (a) The visible-light-excited RTP composite prepared by embedding G-CDs in the B_2O_3 matrix. Reproduced with permission from ref. 68. Copyright 2020, Royal Society of Chemistry. (b) The preparation of visible-light-excited CDs-based RTP composites by using amino acids as carbon sources. Reproduced with permission from ref. 70. Copyright 2023, Elsevier. (c) The N-CDs@PVA material displayed excitation wavelength-dependent RTP upon changing the excitation wavelength from 254 to 470 nm. Reproduced with permission from ref. 65. Copyright 2023, Wiley-VCH.

Although embedding CDs in rigid matrices can offer excellent RTP properties, the introduction of matrices may hinder the applications of CDs-based RTP materials, especially in bioimaging and photodynamic therapy to a certain extent. Thus, some researchers turned to preparing CD-based RTP materials without the assistance of a rigid matrix. Lin and coworkers achieved visible-light-excited matrix-free RTP CDs (AA-CDs) *via* a microwave reaction by taking L-aspartic acid as the carbon precursor (Fig. 9a).[75] The AA-CDs displayed an orange afterglow lasting for about 5s after being irradiated by a commercial blue-light LED (420 nm). Dong and coworkers constructed matrix-free visible-light-excited RTP CDs through a one-step solvothermal reaction utilizing diethylenetriaminepentaacetic acid (EDTA) as the starting raw material (Fig. 9b).[76] The resulting CDs could be excited by accessible LED light sources such as mobile phone flashlights and incandescent lamps, showing yellowish afterglow for about 8 s. Besides, Chen and coauthors rationally chose acrylic acid as the carbon source and ammonium oxalate as the nitrogen source to prepare visible-light-excited RTP CDs *via* a self-matrix strategy.[77] A green RTP emission centered at 476 nm afterglow could be observed after turning off the WLED, displaying a long-lived afterglow for more than 5 s.

Compared with single-color emitting materials, multicolor RTP materials offer superior properties to meet the growing demand for advanced optical applications. Su and Chen *et al.* used thiourea or urea as an ingredient to prepare visible-light-excited multicolor CDs, in which the S and N elements were introduced to improve optical properties.[78] The CDs showed excitation-dependent emission due to the existence of multiple emission centers. Importantly, the absorption was significantly extended to the visible light region with maximum absorption reaching up to 700 nm, which was beneficial to visible-light excitation. Thus, the CDs demonstrated multicolor RTP features, displaying green and yellow emissions after removing irradiation of 365 nm UV light and white light.

In 2022, An and coworkers reported a new family of tunable CDs by a one-pot hydrothermal synthesis of biuret and phosphoric acid (Fig. 10a).[79] Due to the existence of multiple emitting centers, the CDs exhibited excitation-dependent RTP emission, with red-shifted afterglow changing from blue to red upon varying the excitation wavelength from 310 to 440 nm. In the same year, Yang and Zhao *et al.* developed green-light-excitable CD crystals (m,p/CDs-ME) by using *m*-phenylenediamine and phosphoric acid as the starting materials (Fig. 10b).[80] Owing to multiple aggregate states, the m,p/CDs-ME displayed multicolor RTP emission from blue to green under excitation from 200 to 500 nm. Impressively, the lifetime of aqueous suspension of CDs spanned up to 130 ms under green-light excitation (500 nm).

2.5 Other construction strategies

In addition to the above strategies, other feasible methods have been developed for realizing visible-light-excited RTP. Different from the above-mentioned strategies, the reduction of the transitions from the S_0 to the high-lying S_n is also beneficial to achieving visible-light excited RTP materials. Zhu and Zhao *et al.* proposed a rational strategy for achieving visible-light-excited bright RTP materials by multi-esterification of large π-conjugation cores (Fig. 11a).[81] It was found that the multi-esterification of coronene led to a bathochromic shift of the excitation from the UV light to visible light region, which is not only attributed to conjugation extension by an electron-withdrawing ester group, but also due to the boosted transition dipole moment ($\mu_{S_n \rightarrow S_0}$) of low-lying singlet-states. Consequently, efficient visible-light-excited RTP materials were obtained with an ultralong lifetime of up to 2.01 s and an excellent RTP efficiency of 35.4% under blue-light (450 nm) excitation. In addition, these multi-esterified coronene derivatives exhibited long-lived multicolor afterglow lasting over 10 s after the removal of white light.

Host–guest doping is another effective method to realize visible-light-excited RTP. Cai and coworkers realized visible-light-excited NIR RTP emission by rationally utilizing a fused-ring pyrrole-based molecule as a guest and benzophenone (BP) as a host (Fig. 11b).[82] Due to enhanced conjugation in guest molecules, the triplet energy levels greatly dropped and the phosphorescent wavelengths were significantly redshifted from 572 to 764 nm. The phosphorescence emission of 670–720 nm (BP/MAP3) can be observed under excitation at 405 nm using a confocal laser scanning microscope. Also by using a host–guest doping strategy, Liu *et al.* reported visible-light-excited dual-mode emission materials, which could emit

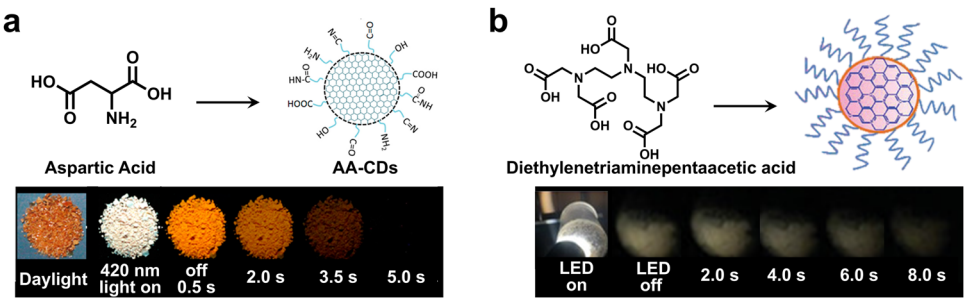

Fig. 9 (a) The visible-light-excited matrix-free RTP CDs prepared by microwave reaction of L-aspartic acid. Reproduced with permission from ref. 75. Copyright 2020, The author(s). (b) The LED-excitable RTP CDs prepared by using EDTA as the raw material. Reproduced with permission from ref. 76. Copyright 2020, Wiley-VCH.

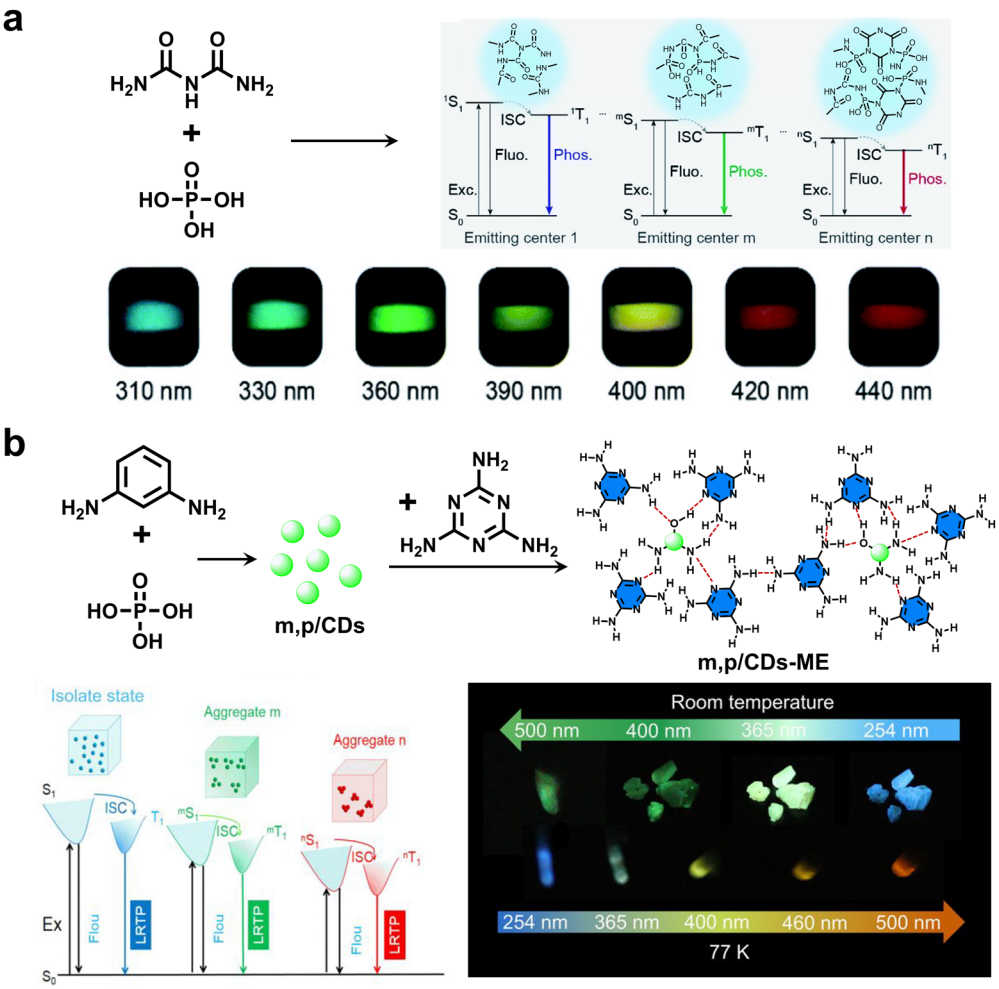

Fig. 10 (a) The preparation of excitation-dependent multicolor CD RTP materials by a one-pot hydrothermal synthesis of biuret and phosphoric acid. Reproduced with permission from ref. 79. Copyright 2022, Royal Society of Chemistry. (b) The synthesis of green-light-excitable CD crystals (m,p/CDs-ME) that exhibited excitation-dependent RTP emission. Reproduced with permission from ref. 80. Copyright 2022, American Chemical Society.

pure white afterglow at 60 °C.[83] Furthermore, the absorption of 6*H*-dibenzo-[*b*,*h*]carbazole (DBCz) reached up to 450 nm with extending conjugation length of guest molecules. As a result, DBCz/Cz can be effectively excited by a white light source with a duration of ~2.5 s.

3. Applications

In the past few years, visible-light-excited RTP materials have been developed rapidly and attracted wide attention in numerous fields such as bioimaging, photodynamic therapy, information encryption, afterglow display and detection due to their unique and abundant luminescence properties. Particularly, visible light sources exhibit lower phototoxicity, deeper penetrability and easy accessibility in comparison with UV light. Thus, visible-light-excited RTP materials have great advantages in actual demand, especially for life-related applications. In this section, we mainly focus on introducing the promising applications of visible-light-excited RTP materials including bioimaging, photodynamic therapy, information encryption and detection.

3.1 Bioimaging

Due to their long lifetimes and large Stokes shifts, RTP materials present a high signal-to-noise ratio (SNR) in bioimaging because they can eliminate the interference of the background fluorescence and autofluorescence from cells or tissues.[82,84,85] Particularly, visible-light excited RTP materials exhibit lower biotoxicity and deeper tissue penetration, thus making them more suitable for bioimaging.

Most of the reported RTP materials are bulk crystals or amorphous films, which are difficult to disperse in water at the nanoscale, greatly limiting their biological applications. Polymer encapsulation is a common strategy for addressing this issue. In 2019, Huang *et al.* demonstrated the outstanding ability of a red metal-free organic phosphor for bioimaging.[86] By using a top-down method, the benzothiadiazole derivative (DBCz-BT) phosphor was encapsulated in an amphiphilic copolymer (F127) to form uniform nanoparticles (5 nm).

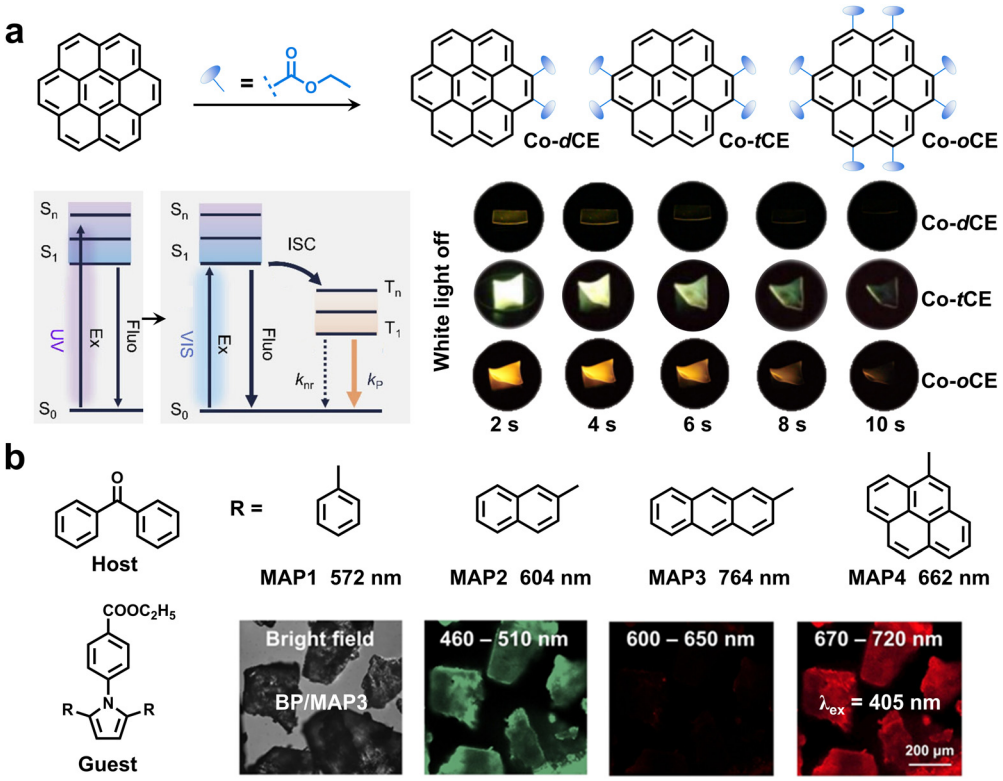

Fig. 11 (a) The strategy of multi-esterification for realizing visible-light-excited RTP materials. Reproduced with permission from ref. 81. Copyright 2023, Wiley-VCH. (b) The preparation of NIR RTP materials by enhancing the conjugation of guest molecules *via* a host–guest doping strategy. Reproduced with permission from ref. 82. Copyright 2023, Wiley-VCH.

Impressively, the nanoparticles exhibited excellent biocompatibility and a long lifetime of 203.1 μs in an aqueous medium, enabling high SNR time-resolved imaging of living HeLa cells and the brain of zebrafish under excitation at 405 nm. Likewise, Huang and Chen *et al.* designed and synthesized a twisted D–A–D phosphor (DCzB) and encapsulated its crystals within F127 to produce nanoparticles for cell imaging (Fig. 12a).[87] The DCzB nanoparticles exhibited tri-mode afterglow of S_1, T_1 and T_1^*, serving as a long-lived cell probe for HeLa cell imaging (λ_{ex} = 405 nm) with a largely enhanced SNR due to the elimination of short-lived autofluorescence interference. Besides, Ma and Tian *et al.* employed TBP@CB[8] for HeLa cell imaging under a 405 nm laser (Fig. 12b).[39] It was found that the bright-yellow afterglow could be observed in the endosomes of cells owing to the aggregation of the TBP@CB[8] complex.

Compared to visible RTP, NIR RTP has a greater penetration depth and lower phototoxicity, which is ideal for practical bioimaging. In 2022, Liu and coworkers developed a family of NIR RTP nanoparticles by a two-step supramolecular assembly, enabling high SNR cell imaging and *in vivo* imaging (Fig. 13a).[88] In the forefront step, a series of alkyl-bridged phenylpyridinium salts were designed and synthesized as guest phosphors. The phenylpyridinium salts were then folded and encapsulated within CB[8], promoting the NIR RTP and two-photon emission due to the TSCT effect. Such host–guest complexes could be further assembled with amphiphilic macrocycle sulfonatocalix[4]arene (SC4AD) to produce uniform ternary nanoparticles with largely enhanced RTP emission. After injection of the as-prepared nanoparticles, the luminescence signal could be clearly observed through the mouse skin without the self-fluorescence interference, benefiting from a higher SNR of NIR phosphorescence. A year later, the same group further reported visible-light-excited NIR RTP for cell and mouse *in vivo* imaging.[89] By using a similar construction strategy, bright NIR RTP emission at 734 nm was realized under excitation at 510 nm, which was highly suitable for high SNR lysosome-target imaging and *in vivo* imaging.

Although the visible-light-excited NIR RTP materials exhibit excellent ability for bioimaging applications, the lifetime is generally very short in the range of microseconds or a few milliseconds. To overcome this issue, Ding and coworkers constructed a series of NIR RTP materials with both long-wavelengths (>600 nm) and ultra-long lifetimes (>100 ms) using a host–guest doping strategy (Fig. 13b).[90] As a proof-of-concept, these host–guest materials demonstrated excellent imaging of lymph nodes and tumors in live mice with a high SNR value of up to 43, benefiting from effectively reducing scattering from tissue and autofluorescence.

3.2 Photodynamic therapy

With multidrug-resistant bacteria posing a serious threat to public health, photodynamic therapy (PDT) has attracted considerable attention due to its non-invasiveness, antibacterial resistance, and so on.[91–94] The singlet oxygen ($^1O_2$) can be produced by the energy transfer (ET) from the triplet excitons

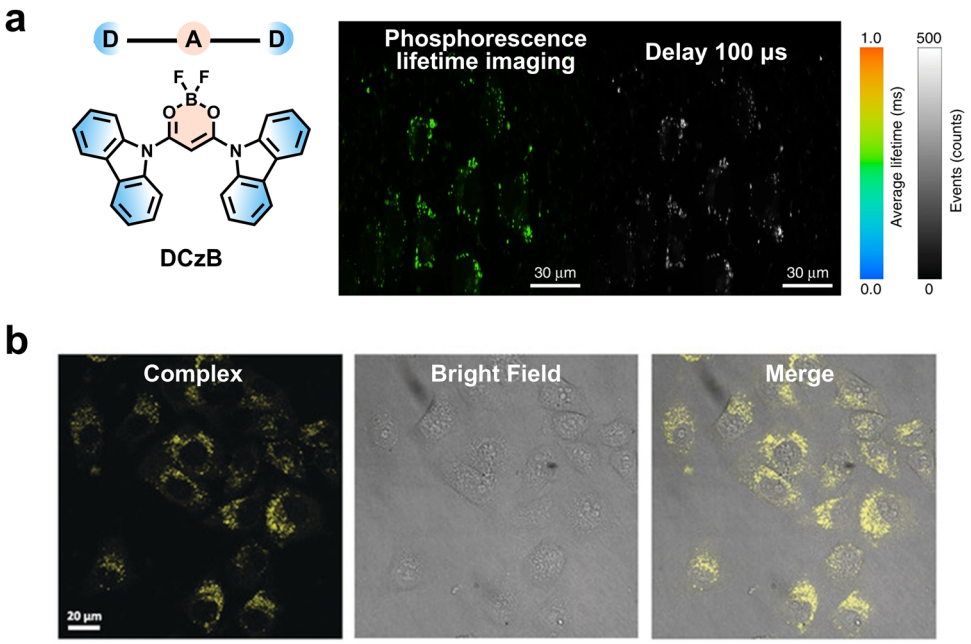

Fig. 12 (a) The preparation of DCzB nanoparticles for cell imaging. Reproduced with permission from ref. 87. Copyright 2020, The author(s). (b) HeLa cell imaging enabled by the TBP@CB[8] complex, λ_{ex} = 405 nm. Reproduced with permission from ref. 39. Copyright 2019, Wiley-VCH.

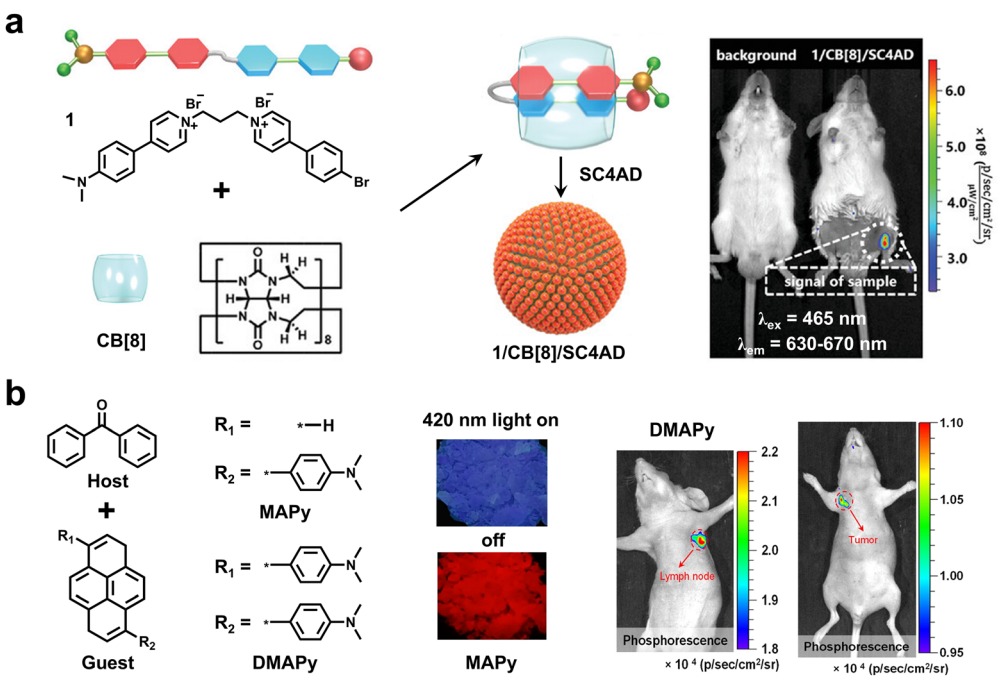

Fig. 13 (a) Two-stage supramolecular assembly to produce spherical NIR RTP nanoparticles for high SNR *in vivo* imaging. Reproduced with permission from ref. 88. Copyright 2022, The author(s). (b) The preparation of ultralong NIR RTP materials using a host–guest doping strategy for high SNR imaging of lymph nodes and tumors in mice. Reproduced with permission from ref. 90. Copyright 2022, The author(s).

to molecular oxygen (O_2), which can be applied to PDT (Fig. 14a). More importantly, the collisional time of ET is greatly prolonged due to the long lifetime of triplet excitons, which leads to high yields of $^1O_2$ to offer excellent therapeutic effects.

In 2020, Huang and coauthors prepared metal-free red-emissive RTP nanoparticles by encapsulating the organic phosphor (DBCz-BT) within F127. The biocompatible RTP nanoparticles revealed a long lifetime of 167 μs in aqueous media and could effectively generate $^1O_2$ to eradicate microorganisms both *in vitro* and *vivo*

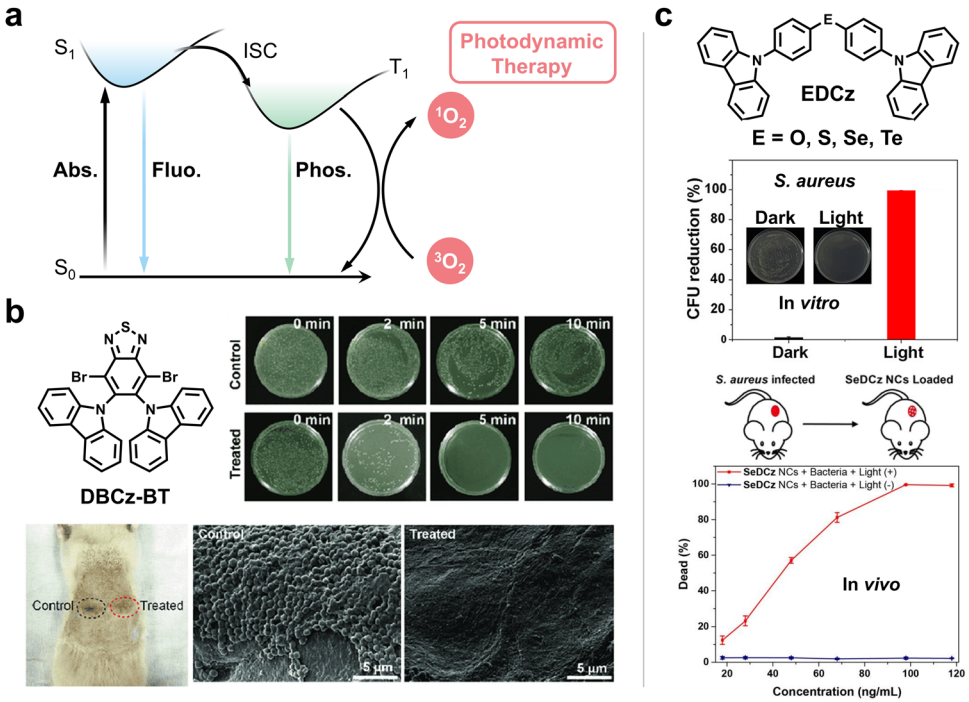

Fig. 14 (a) Simplified Jablonski diagram for illustrating photodynamic therapy. (b) The antimicrobial and anti-infective activity of DBCz-BT *in vitro* and *in vivo* under the 410 nm excitation. Reproduced with permission from ref. 95. Copyright 2019, Springer Nature. (c) The molecular design of chalcogen atom-bridged carbazole derivatives (EDCz) and antibacterial PDT of SeDCz *in vitro* and *vivo* under the white light excitation. Reproduced with permission from ref. 96. Copyright 2020, American Chemical Society.

under visible-light (410 nm) excitation (Fig. 14b).[95] In the same year, He *et al.* designed and synthesized a series of chalcogen atom-bridged carbazole derivatives (EDCz) featuring visible-light-excited RTP emission and demonstrated their outstanding PDT ability *in vivo* and *in vitro* (Fig. 14c).[96] Among these phosphors, SeDCz had the best combination of Φ_P and lifetime, and thus was chosen for PDT studies. The *in vitro* experimental results of the antibacterial demonstrated that the colony-forming units of *S. aureus* were significantly reduced by about 99% in the presence of SeDCz at a very low concentration (98 ng mL^{-1}) under white light irradiation. In a further experiment of PDT *in vivo*, it was found that all *S. aureus* bacteria were killed with the addition of SeDCz (98 ng mL^{-1}) after white light irradiation for 15 min, which is beneficial for wound healing. These results indicated that the SeDCz possesses great potential as a PDT agent.

3.3 Information encryption and anti-counterfeiting

The development of advanced encryption materials is of great significance for combating the escalating issues caused by counterfeit products and information forgery.[97–99] Especially, the RTP materials display unique optical properties including a long lifetime, a large Stokes shift and more dimensionally modulable performance, making them a new generation of optical materials for information storage. It is worth noting that the RTP emission is capable of providing an additional time scale for enhancing the security level of information encryption and anti-counterfeiting. Compared to UV light, visible light is a ubiquitous excitation source and can be accessible from portable LEDs such as flashlights, mobile phones and room light, which contributes to information decoding and validating the authenticity of commodities without any special tools.

Impressively, Huang *et al.* presented visible-light excitable multicolor RTP materials by bridging carbazole and phthalimide units with flexible alkyl chains, which were highly desirable for information encryption.[100] These colorful materials with diverse decay lifetimes were well employed in the 4D information coding. Compared to the traditional 3D code, the new 4D code had an additional time dimension. After ceasing the excitation, a series of tunable codes representing different information at a specific time could be obtained, demonstrating great potential for high-level information security.

Reineke and coworkers developed programmable luminescent tags using visible-light-activatable RTP materials based on the sensitivity of triplet excitons to oxygen (Fig. 15a).[101] By doping phenanthroline derivatives (PhenDpa and PhenTpa) in a rigid PMMA matrix, deep blue light-excitable RTP materials were obtained successfully. Under the irradiation of a 420 nm LED, high-resolution information appeared due to oxygen consumption in the PMMA matrix. And the imprinted information could be reversibly erased by heat. As such, the high-resolution labeling could be effectively written and erased for several cycles based on the activation and deactivation of RTP emission. Differently, Lv and coworkers developed a high-level information encryption system based on visible-light-excited RTP materials.[102] As a proof-of-concept, the digital pattern "321745" was fabricated by two security inks that were prepared

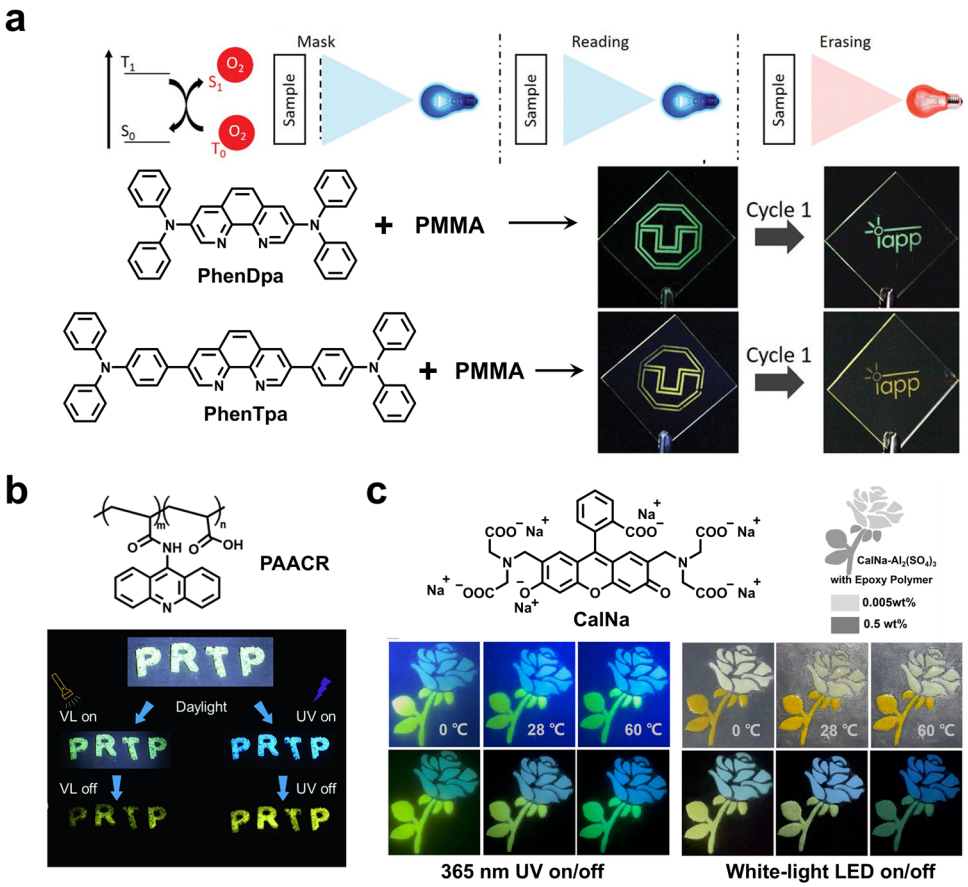

Fig. 15 (a) The writing/erasing of the high-resolution labeling based on photo-activated and deactivated RTP emission. Reproduced with permission from ref. 101. Copyright 2019, Wiley-VCH. (b) Dynamic anti-counterfeiting excited by white light flash and 365 nm UV light based on the PAACR material. Reproduced with permission from ref. 103. Copyright 2024, The author(s). (c) Temperature-dependent anti-counterfeiting patterns enabled by CalNa@$Al_2(SO_4)_3$. Reproduced with permission from ref. 104. Copyright 2022, Wiley-VCH.

by doping phenanthroline derivatives (Aphen) into PVA and PMMA, respectively. Under excitation at 405 nm, all digits are visible. After turning off the 405 nm lamp, only the target digital pattern "3175" written by the Aphen@PVA ink can be observed with strong green afterglow, while "24" written by the Aphen@PMMA ink disappeared due to no afterglow emission.

Recently, Yang and coworkers proposed a covalent coupling strategy to obtain a visible-light excitable RTP material (PAACR) for dynamic anti-counterfeiting (Fig. 15b).[103] The encrypted "PRTP" pattern exhibited the original color of the polymer and blue fluorescence under excitation of visible light and 365 nm UV light, respectively, while displaying yellow afterglow signals after removing the excitation sources. Creatively, Xu and coworkers reported color-tunable dual-mode organic afterglow materials for multi-level anti-counterfeiting (Fig. 15c).[104] The afterglow material CalNa@$Al_2(SO_4)_3$ was prepared by doping an ACQ-type luminogen of calcein sodium (CalNa) into aluminum sulfate, exhibiting dual-mode afterglow emission of TADF and RTP. Such an excellent afterglow material could be efficiently excited by UV or white light and was highly desirable for advanced anti-counterfeiting applications due to the different temperature sensitivity of TADF and RTP. Interestingly, the encrypted rose pattern fabricated by CalNa@$Al_2(SO_4)_3$ exhibited variable colors when the temperature changed from 0 °C to 60 °C after irradiating with a UV lamp or white LED. Hirata *et al.* reported a guideline to enhance luminescence *via* symmetry-breaking molecular motion.[105] The resulting deuterated D–π–D chromophore with efficient red RTP was used to fabricate a star-shaped anti-counterfeiting pattern. The afterglow of the pattern could be clearly observed with unaided eyes after ceasing the ambient light, demonstrating the advantage of the ubiquitous afterglow readout. Taken together, the utilization of RTP materials that can be excited by portable LEDs or ubiquitous room lights has greatly expanded the range of information storage and offered more efficient ways to identify the authenticity of commodities.

3.4 Detection

Afterglow detection exhibits various merits such as a fast response, strong anti-interference ability, high sensitivity and selectivity, easy operation, and low cost.[106] Compared with the other analytical techniques, the long-lived afterglow detection exhibited an improved SNR owing to the effective elimination of autofluorescence and light scattering. Furthermore, RTP materials exhibit abundant responsive properties to specific stimulus sources due to the sensitivity of triplet excitons to the

external environment, which are highly suitable for detection. Lin and coworkers reported robust red RTP materials based on 2D halogen-bonded networks of two maleimide derivatives (DBM and DIM), which could be excited by 500 nm visible light and were highly desirable for detecting toxic heavy metal ions (Fig. 16a).[107] The intensity of RTP emission peak of the DBM film located at around 660 nm exhibited a steady decline upon increasing the concentration of Hg(II) with the detection limit as low as 2.5×10^{-5} nM. The RTP emission could be completely quenched when the concentration of Hg(II) increased up to 10^{-4} M. In contrast, the RTP emission was boosted by 2.2 times after soaking in Cd(II) aqueous. As such, the DBM film could be well applied as an afterglow probe to detect Hg(II) and Cd(II) ions in an aqueous medium with high sensitivity and selectivity.

An *et al.* presented accurate light detection by using excitation-dependent colorful CDs (Fig. 16b).[79] After ceasing excitation light from 310 to 440 nm, distinguishable blue to red afterglow was observed by the naked eye. By establishing the corresponding relationship between the excitation wavelength and the color chart, the excitation wavelength could be identified efficiently and easily in a way of one-to-one correspondence. Besides, Yang and coauthors realized sensitive dopamine detection by leveraging a CD-based RTP material (m,p/CDs-ME), revealing a low detection limit (0.18 μM) and a wide linear range (0–0.04 mM) (Fig. 16c).[80] The phosphorescence intensity displayed a gradually decreasing trend upon increasing the dopamine concentration, along with the quenching efficiency of 89.4% at a concentration of 0.164 mM. More importantly, the RTP probe displayed an excellent anti-interference ability for selective sensing of dopamine in the presence of other amino acids.

Hypoxia detection is beneficial to early diagnosis of various diseases. Wu and coworkers realized ultrasensitive hypoxia detection (K_{SV} = 449.3 bar^{-1}) by using a series of uniform silica nanoparticles (SiNPs).[108] The RTP emission of SiNPs obviously declined at elevated oxygen concentration due to Dexter energy transfer. In further HeLa cell hypoxia monitoring experiments, SiNP-based RTP materials showed visible light/dark differences at different oxygen ratios under 405 nm laser irradiation, demonstrating great potential for hypoxia detection in live cells.

4. Summary and outlook

In the present review, we systematically overviewed recent advances in visible-light-excited RTP materials involving the design and construction strategies, underlying mechanisms, fantastic optical properties and desirable applications. Importantly, several effective strategies have been proposed to construct visible-light-excited RTP materials relying on bathochromic shifts in absorption and inhibition of nonradiative dissipation. Specifically, the strategies of supramolecular aggregation and assembly, charge transfer by D–A design, direct triplet state excitation from S_0 to T_1 and the formation of carbon dots have been proven to be reliable and effective ways to obtain visible-light-excited RTP materials. Besides, other methods such as multi-esterification and deuteration have begun springing up to enhance the afterglow performance. Based on their fantastic optical properties, the visible-light-excited RTP materials have demonstrated excellent

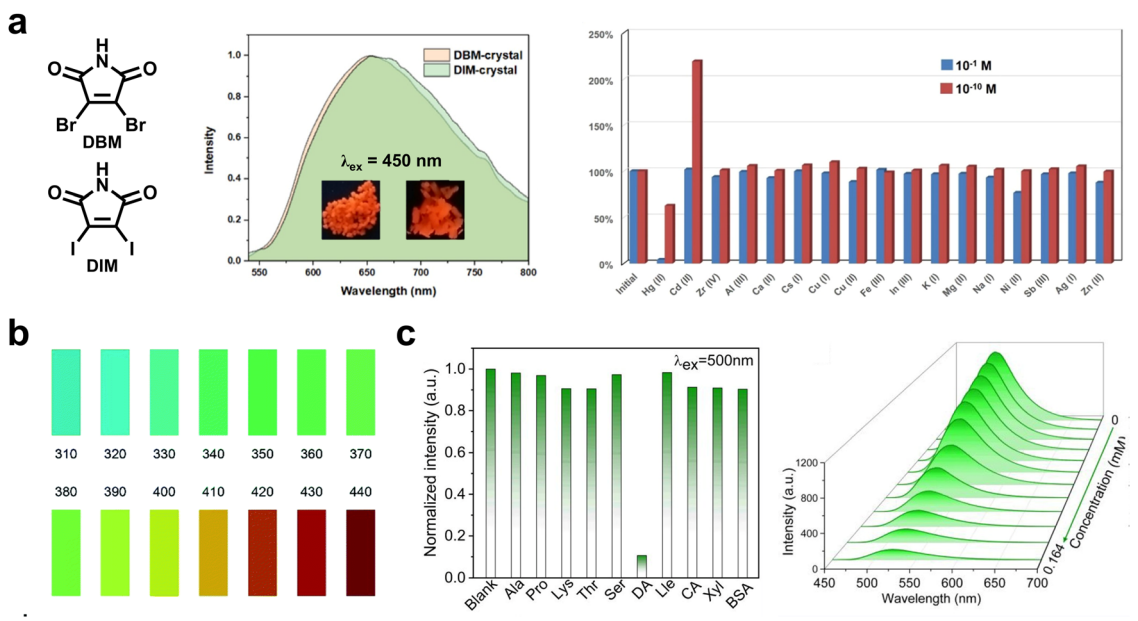

Fig. 16 (a) The visible-light-excited RTP materials (DBM and DIM) enable selective detection of Hg^{2+} and Cd^{2+} in aqueous media. Reproduced with permission from ref. 107. Copyright 2022, American Chemical Society. (b) A standard afterglow color chart established by excitation-dependent multicolor CDs for detecting specific wavelengths from 310 nm to 440 nm. Reproduced with permission from ref. 79. Copyright 2022, Royal Society of Chemistry. (c) Selective detection of dopamine by using m,p/CDs-ME, λ_{ex} = 500 nm. Reproduced with permission from ref. 80. Copyright 2022, American Chemical Society.

potential for application in bioimaging, photodynamic therapy, information encryption, anti-counterfeiting, and detection.

Despite significant progress made in recent years, the study of the visible-light-excited RTP is still in its infancy and faces the following issues and challenges. (i) The universal adaptability and simplicity of the construction strategies should be further improved. How these strategies guide the design and construction of new visible-light-excited RTP materials needs to be analysed in depth; (ii) it is necessary to further elucidate the underlying luminescence mechanisms, which is of great significance for understanding the visible-light excitation and promoting the development of new RTP materials; and (iii) the afterglow properties of visible-light-excited RTP materials need to be further enhanced. The long lifetime, high quantum yield, and NIR emission are essentially important for practical applications such as afterglow displays and bioimaging. Especially, most of the high-efficiency NIR RTP materials relied on transition-metal-based complexes. Effective preparation methods still need to be further explored to obtain purely organic NIR RTP materials; and (iv) more efforts should be devoted to expanding the application scope of the visible-light-excited RTP materials. The related RTP materials are highly desirable and applicable in various fields such as afterglow displays, biocompatible imaging, sensitive and portable sensing, and information storage. Such studies will largely promote the development of visible-light-excited RTP. With increasing contributions from multifaceted researchers, we believe that a boom in the field of visible-light-excited RTP is surely forthcoming.

Data availability

Data availability is not applicable to this article as no new data were created or analyzed in this study.

Conflicts of interest

There are no conflicts of interest to declare.

Acknowledgements

This project was financially supported by the National Natural Science Foundation of China (22205249), Natural Science Foundation of Zhejiang Province (LQ23B040002 and LD22E050008), Sino-German Mobility Program (M-0424), and International Cooperation Project of Ningbo City (2023H019). The authors also thanked Prof. Patrick Théato from the Karlsruhe Institute of Technology for his thoughtful suggestions.

References

1 W. Zhao, Z. He and B. Z. Tang, *Nat. Rev. Mater.*, 2020, **5**, 869–885.
2 B. Chang, J. Chen, J. Bao, T. Sun and Z. Cheng, *Chem. Rev.*, 2023, **123**, 13966–14037.
3 X. Wang, H. F. Shi, H. L. Ma, W. P. Ye, L. L. Song, J. Zan, X. K. Yao, X. Y. Ou, G. H. Yang, Z. Zhao, M. Singh, C. Y. Lin, H. Wang, W. Y. Jia, Q. Wang, J. H. Zhi, C. M. Dong, X. Y. Jiang, Y. G. Tang, X. J. Xie, Y. Yang, J. P. Wang, Q. S. Chen, Y. Wang, H. H. Yang, G. Q. Zhang, Z. F. An, X. G. Liu and W. Huang, *Nat. Photonics*, 2021, **15**, 187–192.
4 X. Su, X. Kong, K. Sun, Q. Liu, Y. Pei, D. Hu, M. Xu, W. Feng and F. Li, *Angew. Chem., Int. Ed.*, 2022, **61**, e202201630.
5 H. Chen, Y. Sun, M. Liu, F. Li, Q. Peng and H. Huang, *Angew. Chem., Int. Ed.*, 2023, **62**, e202302629.
6 Y. Zhou, W. Qin, C. Du, H. Gao, F. Zhu and G. Liang, *Angew. Chem., Int. Ed.*, 2019, **58**, 12102–12106.
7 Y. Zhou, L. Jin, J. Chen, W. Hong, G. Liang and W. Qin, *Chem. Eng. J.*, 2023, **463**, 142506.
8 W. Ye, H. Ma, H. Shi, H. Wang, A. Lv, L. Bian, M. Zhang, C. Ma, K. Ling, M. Gu, Y. Mao, X. Yao, C. Gao, K. Shen, W. Jia, J. Zhi, S. Cai, Z. Song, J. Li, Y. Zhang, S. Lu, K. Liu, C. Dong, Q. Wang, Y. Zhou, W. Yao, Y. Zhang, H. Zhang, Z. Zhang, X. Hang, Z. An, X. Liu and W. Huang, *Nat. Mater.*, 2021, **20**, 1539–1544.
9 T. Wang, X. Su, X. Zhang, X. Nie, L. Huang, X. Zhang, X. Sun, Y. Luo and G. Zhang, *Adv. Mater.*, 2019, **31**, 1904273.
10 L. Li, J. Zhou, J. Han, D. Liu, M. Qi, J. Xu, G. Yin and T. Chen, *Nat. Commun.*, 2024, **15**, 3846.
11 G. Q. Yin, J. Y. Zhou, W. Lu, L. Q. Li, D. P. Liu, M. Qi, B. Z. Tang, P. Théato and T. Chen, *Adv. Mater.*, 2024, DOI: **10.1002/adma.202311347**.
12 Y. Zhang, Y. Su, H. Wu, Z. Wang, C. Wang, Y. Zheng, X. Zheng, L. Gao, Q. Zhou, Y. Yang, X. Chen, C. Yang and Y. Zhao, *J. Am. Chem. Soc.*, 2021, **143**, 13675–13685.
13 X. Zheng, Q. Han, Q. Lin, C. Li, J. Jiang, Q. Guo, X. Ye, W. Z. Yuan, Y. Liu and X. Tao, *Mater. Horiz.*, 2023, **10**, 197–208.
14 L. Gao, J. Huang, L. Qu, X. Chen, Y. Zhu, C. Li, Q. Tian, Y. Zhao and C. Yang, *Nat. Commun.*, 2023, **14**, 7252.
15 G. Yin, G. Huo, M. Qi, D. Liu, L. Li, J. Zhou, X. Le, Y. Wang and T. Chen, *Adv. Funct. Mater.*, 2023, **34**, 2310043.
16 Y. He, J. Wang, Q. Li, S. Qu, C. Zhou, C. Yin, H. Ma, H. Shi, Z. Meng and Z. An, *Adv. Opt. Mater.*, 2023, **11**, 2201641.
17 D. Wang, H. Wu, J. Gong, Y. Xiong, Q. Wu, Z. Zhao, L. Wang, D. Wang and B. Z. Tang, *Mater. Horiz.*, 2022, **9**, 1081–1088.
18 Z. Xie, X. Zhang, H. Wang, C. Huang, H. Sun, M. Dong, L. Ji, Z. An, T. Yu and W. Huang, *Nat. Commun.*, 2021, **12**, 3522.
19 Z. Wu, K. Bergmann and Z. M. Hudson, *Angew. Chem., Int. Ed.*, 2024, **63**, e202319089.
20 Z. Wu, H. Choi and Z. M. Hudson, *Angew. Chem., Int. Ed.*, 2023, **62**, e202301186.
21 H. Zhu, I. Badía-Domínguez, B. Shi, Q. Li, P. Wei, H. Xing, M. C. Ruiz Delgado and F. Huang, *J. Am. Chem. Soc.*, 2021, **143**, 2164–2169.
22 S. Garain, S. N. Ansari, A. A. Kongasseri, B. Chandra Garain, S. K. Pati and S. J. George, *Chem. Sci.*, 2022, **13**, 10011–10019.

23 M. Singh, K. Shen, W. Ye, Y. Gao, A. Lv, K. Liu, H. Ma, Z. Meng, H. Shi and Z. An, *Angew. Chem., Int. Ed.*, 2024, **63**, e202319694.
24 Z. Zhao, Y. Cai, Q. Zhang, A. Li, T. Zhu, X. Chen and W. Z. Yuan, *Nat. Commun.*, 2024, **15**, 5054.
25 S. Y. Zheng, T. W. Zhu, Y. Z. Wang, T. J. Yang and W. Z. Yuan, *Angew. Chem., Int. Ed.*, 2020, **59**, 10018–10022.
26 X. Liu, Q. Liao, J. Yang, Z. Li and Q. Li, *Angew. Chem., Int. Ed.*, 2023, **62**, e202302792.
27 G. Yin, W. Lu, J. Huang, R. Li, D. Liu, L. Li, R. Zhou, G. Huo and T. Chen, *Aggregate*, 2023, **4**, e344.
28 X.-F. Wang, H. Xiao, P.-Z. Chen, Q.-Z. Yang, B. Chen, C.-H. Tung, Y.-Z. Chen and L.-Z. Wu, *J. Am. Chem. Soc.*, 2019, **141**, 5045–5050.
29 Y. Fan, S. Liu, M. Wu, L. Xiao, Y. Fan, M. Han, K. Chang, Y. Zhang, X. Zhen, Q. Li and Z. Li, *Adv. Mater.*, 2022, **34**, 2201208.
30 B. Wu, N. N. Guo, X. T. Xu, Y. M. Xing, K. Shi, W. H. Fang and G. J. Wang, *Adv. Opt. Mater.*, 2020, **8**, 2001192.
31 M. Wohlgenannt and Z. V. Vardeny, *J. Phys.: Condens. Matter*, 2003, **15**, R83–R107.
32 X.-K. Ma and Y. Liu, *Acc. Chem. Res.*, 2021, **54**, 3403–3414.
33 J. Yang, Y. Zhang, X. Wu, W. Dai, D. Chen, J. Shi, B. Tong, Q. Peng, H. Xie, Z. Cai, Y. Dong and X. Zhang, *Nat. Commun.*, 2021, **12**, 4883.
34 Z. An, C. Zheng, Y. Tao, R. Chen, H. Shi, T. Chen, Z. Wang, H. Li, R. Deng, X. Liu and W. Huang, *Nat. Mater.*, 2015, **14**, 685–690.
35 Q. Liao, Q. Li and Z. Li, *Adv. Mater.*, 2023, DOI: **10.1002/adma.202306617**.
36 S. Cai, X. Yao, H. Ma, H. Shi and Z. An, *Aggregate*, 2023, **4**, e320.
37 S. Cai, H. Shi, J. Li, L. Gu, Y. Ni, Z. Cheng, S. Wang, W. W. Xiong, L. Li, Z. An and W. Huang, *Adv. Mater.*, 2017, **29**, 1701244.
38 D. Guo, W. Wang, K. Zhang, J. Chen, Y. Wang, T. Wang, W. Hou, Z. Zhang, H. Huang, Z. Chi and Z. Yang, *Nat. Commun.*, 2024, **15**, 3598.
39 J. Wang, Z. Huang, X. Ma and H. Tian, *Angew. Chem., Int. Ed.*, 2020, **59**, 9928–9933.
40 X. Nie, J. Du, W. Huang, T. Wang, X. Wang, B. Chen, X. Zhang and G. Zhang, *Adv. Opt. Mater.*, 2022, **10**, 2200099.
41 J. You, X. Zhang, Q. Nan, K. Jin, J. Zhang, Y. Wang, C. Yin, Z. Yang and J. Zhang, *Nat. Commun.*, 2023, **14**, 4163.
42 G. Yong, X. Zhang and W. She, *Dyes Pigm.*, 2013, **97**, 65–70.
43 Y. Zhao, G. Yong, X. Zhang and B. Zhang, *Dyes Pigm.*, 2014, **101**, 172–178.
44 D. Tu, S. Cai, C. Fernandez, H. Ma, X. Wang, H. Wang, C. Ma, H. Yan, C. Lu and Z. An, *Angew. Chem., Int. Ed.*, 2019, **58**, 9129–9133.
45 T. Zhang, X. Ma and H. Tian, *Chem. Sci.*, 2020, **11**, 482–487.
46 S. Sun, L. Ma, J. Wang, X. Ma and H. Tian, *Natl. Sci. Rev.*, 2022, **9**, nwab085.
47 Q. Xu, L. Ma, S. Sun and X. Ma, *J. Mater. Chem. C*, 2021, **9**, 14623–14627.
48 Y. Luo, Z. Pang, C. Li, K. Chen, X. Zheng, Y. Huang and Z. Lu, *J. Mater. Chem. C*, 2020, **8**, 11603–11609.
49 Y. Huang, X. Zheng, Z. Yao, W. Lv, S. Xiang, Q. Ling and Z. Lin, *Chem. Eng. J.*, 2022, **444**, 136629.
50 H. Bhatia and D. Ray, *J. Phys. Chem. C*, 2019, **123**, 22104–22113.
51 X. F. Wang, W. J. Guo, H. Xiao, Q. Z. Yang, B. Chen, Y. Z. Chen, C. H. Tung and L. Z. Wu, *Adv. Funct. Mater.*, 2020, **30**, 1907282.
52 J. Jin, P. Xue, L. Zhang, H. Jiang, W. Wang, Q. Yang, Y. Tao, C. Zheng, R. Chen and W. Huang, *Angew. Chem., Int. Ed.*, 2021, **60**, 24984–24990.
53 Y. Wang, Q. Sun, L. Yue, J. Ma, S. Yuan, D. Liu, H. Zhang, S. Xue and W. Yang, *Adv. Opt. Mater.*, 2021, **9**, 2101075.
54 J. Yuan, R. Chen, X. Tang, Y. Tao, S. Xu, L. Jin, C. Chen, X. Zhou, C. Zheng and W. Huang, *Chem. Sci.*, 2019, **10**, 5031–5038.
55 J. Yuan, Y. Wang, B. Zhou, W. Xie, B. Zheng, J. Zhang, P. Li, T. Yu, Y. Qi, Y. Tao and R. Chen, *Molecules*, 2024, **29**, 1014.
56 Y. Wang, Z. Zhang, L. Liu, S. Yuan, J. Ma, D. Liu, S. Xue, Q. Sun and W. Yang, *J. Mater. Chem. C*, 2019, **7**, 9671–9677.
57 C. Chen, Z. Chi, K. C. Chong, A. S. Batsanov, Z. Yang, Z. Mao, Z. Yang and B. Liu, *Nat. Mater.*, 2021, **20**, 175–180.
58 J. Chavez, L. Ceresa, E. Kitchner, J. Kimball, T. Shtoyko, R. Fudala, J. Borejdo, Z. Gryczynski and I. Gryczynski, *J. Photochem. Photobiol., B*, 2020, **208**, 111897.
59 S. Y. Lim, W. Shen and Z. Gao, *Chem. Soc. Rev.*, 2015, **44**, 362–381.
60 X. He, Y. Zheng, C. Hu, B. Lei, X. Zhang, Y. Liu and J. Zhuang, *Mater. Horiz.*, 2024, **11**, 113–133.
61 H. Shi, Y. Wu, J. Xu, H. Shi and Z. An, *Small*, 2023, **19**, 2207104.
62 H. Wu, Y. Kang, S. Jiang, K. Wang, L. Qu and C. Yang, *Small*, 2024, DOI: **10.1002/smll.202402796**.
63 K. Zheng, X. Li, M. Chen, Y. Gong, A. Tang, Z. Wang, Z. Wei, L. Guan and F. Teng, *Chem. Eng. J.*, 2020, **380**, 122503.
64 J. Yu, X. Yong, Z. Tang, B. Yang and S. Lu, *J. Phys. Chem. Lett.*, 2021, **12**, 7671–7687.
65 B. Xu, Y. Jia, H. Ning, Q. Teng, C. Li, X. Fang, J. Li, H. Zhou, X. Meng, Z. Gao, X. Wang, Z. Wang and F. Yuan, *Small*, 2023, **20**, 2304958.
66 B. Wang and S. Lu, *Matter*, 2022, **5**, 110–149.
67 S. Xue, P. Li, L. Sun, L. An, D. Qu, X. Wang and Z. Sun, *Small*, 2023, **19**, e2206180.
68 Z. Xu, X. Sun, P. Ma, Y. Chen, W. Pan and J. Wang, *J. Mater. Chem. C*, 2020, **8**, 4557–4563.
69 W. He, X. Sun and X. Cao, *ACS Sustainable Chem. Eng.*, 2021, **9**, 4477–4486.
70 Y. Huang and P. Li, *Chem. Eng. J.*, 2024, **480**, 148157.
71 M. Cheng, P. Wang, L. Cao, W.-F. Dong, L. Li and R. Yan, *J. Lumin.*, 2022, **252**, 119370.
72 Q. Li, Z. Zhao, S. Meng, Y. Li, Y. Zhao, B. Zhang, Z. Tang, J. Tan and S. Qu, *SmartMat*, 2021, **3**, 260–268.
73 H. Wang, B. Shi, H. Yu, S. Yang, G. Nie, S. Wang and W. Chen, *Mater. Today Adv.*, 2023, **20**, 100429.

74 W. Sun, W. Hu, B. Shi and C. Lü, *J. Lumin.*, 2023, **263**, 120078.
75 S. Hu, K. Jiang, Y. Wang, S. Wang, Z. Li and H. Lin, *Nanomaterials*, 2020, **10**, 464.
76 Y. Gao, H. Zhang, S. Shuang and C. Dong, *Adv. Opt. Mater.*, 2020, **8**, 1901557.
77 H. Wang, H. Yu, A. Al-Zubi, X. Zhu, G. Nie, S. Wang and W. Chen, *Nanomaterials*, 2022, **12**, 2210.
78 W. Wang, R. Mei, Q. Zhao, C. Liu, H. Chen, S. Su and S. Wang, *J. Phys. Chem. Lett.*, 2022, **13**, 726–732.
79 H. Shi, Z. Niu, H. Wang, W. Ye, K. Xi, X. Huang, H. Wang, Y. Liu, H. Lin, H. Shi and Z. An, *Chem. Sci.*, 2022, **13**, 4406–4412.
80 Y. Zheng, Z. Wang, J. Liu, Y. Zhang, L. Gao, C. Wang, X. Zheng, Q. Zhou, Y. Yang, Y. Li, H. Tang, L. Qu, Y. Zhao and C. Yang, *ACS Appl. Mater. Interfaces*, 2022, **14**, 15706–15715.
81 J. Yu, Z. Sun, H. Ma, C. Wang, W. Huang, Z. He, W. Wu, H. Hu, W. Zhao and W. H. Zhu, *Angew. Chem., Int. Ed.*, 2023, **62**, e202316647.
82 Y. Zhao, J. Yang, C. Liang, Z. Wang, Y. Zhang, G. Li, J. Qu, X. Wang, Y. Zhang, P. Sun, J. Shi, B. Tong, H. Y. Xie, Z. Cai and Y. Dong, *Angew. Chem., Int. Ed.*, 2023, **63**, e202317431.
83 X. Zhang, K. C. Chong, Z. Xie and B. Liu, *Angew. Chem., Int. Ed.*, 2023, **62**, e202310335.
84 Q. Dang, Y. Jiang, J. Wang, J. Wang, Q. Zhang, M. Zhang, S. Luo, Y. Xie, K. Pu, Q. Li and Z. Li, *Adv. Mater.*, 2020, **32**, 2006752.
85 K. Chang, L. Y. Xiao, Y. Y. Fan, J. Q. Gu, Y. S. Wang, J. Yang, M. Z. Chen, Y. F. Zhang, Q. Q. Li and Z. Li, *Sci. Adv.*, 2023, **9**, eadf6757.
86 H. Shi, L. Zou, K. Huang, H. Wang, C. Sun, S. Wang, H. Ma, Y. He, J. Wang, H. Yu, W. Yao, Z. An, Q. Zhao and W. Huang, *ACS Appl. Mater. Interfaces*, 2019, **11**, 18103–18110.
87 J. Jin, H. Jiang, Q. Yang, L. Tang, Y. Tao, Y. Li, R. Chen, C. Zheng, Q. Fan, K. Y. Zhang, Q. Zhao and W. Huang, *Nat. Commun.*, 2020, **11**, 842.
88 X. K. Ma, X. Zhou, J. Wu, F. F. Shen and Y. Liu, *Adv. Sci.*, 2022, **9**, 2201182.
89 H.-J. Wang, M.-M. Zheng, W.-W. Xing, Y.-X. Li, Y.-Y. Wang, H. Zhu, Y.-M. Zhang, Q. Yu and Y. Liu, *Chem. Sci.*, 2023, **14**, 8401–8407.
90 F. Xiao, H. Gao, Y. Lei, W. Dai, M. Liu, X. Zheng, Z. Cai, X. Huang, H. Wu and D. Ding, *Nat. Commun.*, 2022, **13**, 186.
91 X. Wang, W. Sun, H. Shi, H. Ma, G. Niu, Y. Li, J. Zhi, X. Yao, Z. Song, L. Chen, S. Li, G. Yang, Z. Zhou, Y. He, S. Qu, M. Wu, Z. Zhao, C. Yin, C. Lin, J. Gao, Q. Li, X. Zhen, L. Li, X. Chen, X. Liu, Z. An, H. Chen and W. Huang, *Nat. Commun.*, 2022, **13**, 5091.
92 Z. Xu, Y. Jiang, Y. Shen, L. Tang, Z. Hu, G. Lin, W.-C. Law, M. Ma, B. Dong, K.-T. Yong, G. Xu, Y. Tao, R. Chen and C. Yang, *Mater. Horiz.*, 2022, **9**, 1283–1292.
93 G. Feng, G.-Q. Zhang and D. Ding, *Chem. Soc. Rev.*, 2020, **49**, 8179–8234.
94 X. Ma, Y. Liu, S. Li, K. Ogino, R. Xing and X. Yan, *Supramolecular Mat.*, 2022, **1**, 100010.
95 S. Wang, M. Xu, K. Huang, J. Zhi, C. Sun, K. Wang, Q. Zhou, L. Gao, Q. Jia, H. Shi, Z. An, P. Li and W. Huang, *Sci. China Mater.*, 2019, **63**, 316–324.
96 L. Xu, K. Zhou, H. Ma, A. Lv, D. Pei, G. Li, Y. Zhang, Z. An, A. Li and G. He, *ACS Appl. Mater. Interfaces*, 2020, **12**, 18385–18394.
97 H. Shang, X. Le, Y. Sun, S. Wu, Y. Wang, P. Theato and T. Chen, *Mater. Horiz.*, 2024, **11**, 2856–2864.
98 J. Li, S. Xie, J. Meng, Y. Liu, Q. Zhan, Y. Zhang, L. Shui, G. Zhou, B. L. Feringa and J. Chen, *CCS Chem.*, 2024, **6**, 427–438.
99 H. Zhang, H. Liu, Z. Hu and X. Ji, *Supramolecular Mat.*, 2022, **1**, 100018.
100 X. Wang, H. L. Ma, M. X. Gu, C. Q. Lin, N. Gan, Z. L. Xie, H. Wang, L. F. Bian, L. S. Fu, S. Z. Cai, Z. G. Chi, W. Yao, Z. F. An, H. F. Shi and W. Huang, *Chem. Mater.*, 2019, **31**, 5584–5591.
101 M. Louis, H. Thomas, M. Gmelch, A. Haft, F. Fries and S. Reineke, *Adv. Mater.*, 2019, **31**, 1807887.
102 W. Sun, B. Shi, Z. Xia and C. Lü, *Mater. Today Chem.*, 2023, **27**, 101297.
103 Q. Chen, L. Qu, H. Hou, J. Huang, C. Li, Y. Zhu, Y. Wang, X. Chen, Q. Zhou, Y. Yang and C. Yang, *Nat. Commun.*, 2024, **15**, 2947.
104 Y. Liang, C. Xu, H. Zhang, S. Wu, J. A. Li, Y. Yang, Z. Mao, S. Luo, C. Liu, G. Shi, F. Sun, Z. Chi and B. Xu, *Angew. Chem., Int. Ed.*, 2023, **62**, e202217616.
105 B. Sk and S. Hirata, *Adv. Sci.*, 2024, **11**, 2308897.
106 S. Tao, S. Lu, Y. Geng, S. Zhu, S. A. T. Redfern, Y. Song, T. Feng, W. Xu and B. Yang, *Angew. Chem., Int. Ed.*, 2018, **57**, 2393–2398.
107 S. Wang, J. Wang, Q. Huang, X. Zheng, Z. Yao, S. Xiang, Q. Ling and Z. Lin, *ACS Appl. Mater. Interfaces*, 2022, **14**, 14703–14711.
108 T. He, W. J. Guo, Y. Z. Chen, X. F. Yang, C. H. Tung and L. Z. Wu, *Aggregate*, 2022, **4**, e250.